https://doi.org/10.5194/egusphere-2026-3369
Preprint. Discussion started: 22 July 2026

Mid-Century Projections of Waves and Water Levels Highlight the Dominant Role of Sea-Level Rise in the Salish Sea

Kai Parker[1], Kees Nederhoff[2], Anita Engelstad[3], Eric Grossman[4], Li Erikson[5]

[1] USGS, Pacific Coastal and Marine Science Center, Santa Cruz, USA. (kaparker@usgs.gov) ORCID-ID: 0000-0002-0268-3891
[2] Deltares USA, 8601 Georgia Ave., Silver Spring, MD 20910, USA, (kees.nederhoff@deltares-usa.us) ORCID-ID: 0000-0003-0552-3428
[3] USGS, Pacific Coastal and Marine Science Center, Santa Cruz, USA. (aengelstad@usgs.gov) ORCID-ID:
[4] USGS, Pacific Coastal and Marine Science Center, Santa Cruz, USA. (egrossman@usgs.gov) ORCID-ID: 0000-0003-1414-6476
[5] USGS, Pacific Coastal and Marine Science Center, Santa Cruz, USA. (lerikson@usgs.gov) ORCID-ID: https://orcid.org/0000-0002-8607-7695

Correspondence to: Kai Parker (kaip461@ecy.wa.gov)

Abstract:

Using high-resolution, ensemble-based modeling of the CMIP6 High Resolution Model Intercomparison Project, this study evaluates potential changes to extreme coastal water levels and waves across the Salish Sea, the largest estuary on the North American west coast. Results of a well-validated (water level error ~10 cm) regional hydrodynamic and wave model indicate that extreme water levels (e.g., 30-year return period) are projected to increase across the region, while lower-magnitude events (e.g., annual) are projected to slightly decrease. Wave height projections are spatially heterogeneous but generally decrease in southern basins and increase in the far north basins. Seasonal decomposition reveals a modest decrease in winter water levels and an increase in summer water levels. Non-linear interactions between sea level rise (SLR) and hydrodynamic response were assessed across seven SLR scenarios (0–3 m), revealing localized amplification effects up to 10 cm, though these remain minor relative to the SLR signal. Overall, uncertainty across the CMIP6 ensemble is high in this region, rendering most modeled changes

https://doi.org/10.5194/egusphere-2026-3369
Preprint. Discussion started: 22 July 2026

statistically non-significant and emphasizing the need for studies to consider an ensemble when looking at climate projections. The dominance of tidal forcing in extreme water levels, coupled with high inter-model variability, indicates that near-term climate-induced changes to oceanic drivers are unlikely to significantly alter coastal hazards in the Salish Sea by 2050. These findings support the use of present-day conditions as a proxy for near-future planning and emphasize SLR as the primary contributor to changing future coastal risk in the Salish Sea.

Keywords: Extreme Sea levels, Coastal Flooding, Regional Hindcast, Wave Setup, Water Levels, Extreme Events,

1. **Introduction**

Communities are increasingly dealing with the challenge of planning for coastal hazards as sea level rise (SLR) and changing climate establish a new coastal baseline. Changes in dynamics and hazards are already being observed globally (IPCC, 2021), and the world's coastlines will experience significant changes in the coming decades and centuries (McMichael et al., 2020). In response, communities increasingly seek to incorporate climate-related changes into planning and management. However, these efforts are often constrained by limited data, analytical capacity, or access to scientific expertise. Because adaptation decisions can involve substantial investments of time and resources, there is a growing need for robust, decision-relevant scientific information that can support communities as they evaluate their options.

To support more comprehensive planning, we evaluate the effect of climate change on regional water levels and waves in the Salish Sea. The Salish Sea, spanning the border of Washington, United States of America, and British Columbia, Canada, is one of the largest inland seas in the world and is densely populated with a coastal population of around 8.7 million. The region is projected to continue to grow by an additional 5 million by 2040, with much of this growth expected in low elevation regions (Sobocinski, 2021). This high level of urbanization is paired with a relatively dynamic climate. While most of the Salish Sea is at least partially shielded from Pacific Ocean storms, extratropical cyclones bring extreme

https://doi.org/10.5194/egusphere-2026-3369
Preprint. Discussion started: 22 July 2026

winds comparable in strength to hurricanes and intense rain to the region. The region also features mesotidal tides and large river systems, both of which commonly drive flooding.

Coastal hazards in the Salish Sea have been recognized for decades. As an example, over 1/3 of the Salish Sea's coastline has been armored (Shipman et al., 2010), and this percentage can even reach over 80% for more urbanized areas (King County, 2019). Most of the coastal ecosystem has been modified (Simenstad et al., 2011), and an extensive system of dikes, levees, and other flood control infrastructure crisscross the coastal lowlands. That said, formal information on coastal hazards and storm surge in the Salish Sea has been slow to develop. Few studies have systematically explored drivers of coastal flooding across the region, and even fewer studies have examined how these drivers may change in the future. Recent work has used numerical modeling to explore the development of surge during extreme events, with all highlighting the importance of remote water level anomalies and the variability in response of coastal waters across the Salish Sea (Abeysirigunawardena et al., 2011; Grossman et al., 2023; Soontiens et al., 2016; Yang et al., 2020). The progression of science summarized in University of Washington's Climate Impacts Group (CIG) (2005) to CIG (2015) regarding the state of climate change knowledge in the Puget Sound shows a growing consensus of climate change impacts in the region but indicates that many gaps remain. In terms of coastal hazard drivers, some consensus has been reached regarding how streamflow and SLR will impact the region. Less is understood about oceanic forcing, such as the extent that storm surge and/or waves will be affected by climate change. Hamman (2012) explored the effects of climate on the Skagit and Nisqually River Basins and found minimal change in future storm forcing as predicted by a downscaled CMIP3 model.

This study builds upon the foundation of Hamman (2012) by better characterizing storms and waves across the Salish Sea. This is accomplished first by integrating new high-resolution CMIP6 climate forecast ensembles. The latest CMIP6 ensemble provides increased spatial and temporal resolution and more accurate simulations of the physics (e.g., improved air-sea flux formulations and better representation of convection and precipitation), allowing for a better representation of extremes, improved regional scale information, and ideally decreased inter-modal variability (Eyring et al., 2019; Chen et al.,

https://doi.org/10.5194/egusphere-2026-3369
Preprint. Discussion started: 22 July 2026

2020). In terms of horizontal resolution, this study benefits from General Circulation Models (GCMs) moving from ~ 200 km (CMIP5) to under 50 km (CMIP6 High Resolution). Leveraging an ensemble of these new, state-of-the-science datasets enables more robust analysis of projected changes in regional water levels and waves for the near future climate trajectory. These data are then used to force regional models, providing information across the entire Salish Sea. Often coastal data are fragmented, containing gaps and providing an incomplete or inhomogeneous record that is unusable for large-scale planning or strategic resource allocation. This study addresses this problem by providing a scientifically robust analysis that is usable across the U.S. portion of the Salish Sea region. Finally, this study delineates the relative contribution of processes and their relevance for future work. For example, information on the magnitude and significance of climate change impacts to forcing (e.g., waves and water levels) provides guidance about relevance for future studies. Such information, particularly when it supports assumptions, validates simplifications, or quantifies future uncertainties, can be used for coastal hazard and process studies, and allows resources and methodologies to be optimally allocated.

2. Study Sites and Data

2.1 Study Region

This study is focused on the U.S. waters of the Salish Sea, a large inland sea opening onto the northeast Pacific Ocean and located at the border between the United States and Canada (Figure 1). The Salish Sea is a complex fjordic estuarine system composed of many branches, islands, channels, and large, deep basins. Tides in the Salish Sea are mixed-semidiurnal or mixed-diurnal with considerable variability in amplitude and phase across the region. For example, mean tide range increases from 1.7 m at Neah Bay to 3.2 m at Olympia (Mofjeld & Larsen, 1984). The large tidal prism of the Salish Sea can produce strong tidal currents (in excess of 1 m/s) in channels and inlets and weaker currents in basins (Stevens et al., 2012). Many rivers enter the sea, providing significant freshwater input and help create a strong gradient in salinity, temperature, and density (MacCready and Geyer, 2024).

https://doi.org/10.5194/egusphere-2026-3369
Preprint. Discussion started: 22 July 2026

Storm events in the Salish Sea are primarily driven by extratropical cyclones originating in the eastern Pacific Ocean. Vancouver Island and the Olympic Peninsula provide some shielding for the inner sea, but significant surge is still induced by the combination of strong winds (Abeysirigunawardena et al., 2009) and low pressures (Thomson et al., 2009). Maximum surge levels are generally in the range of 0.8 to 1.0 m (Yang et al., 2019). In addition to locally generated surge, multiple studies have highlighted the importance of remote sea surface anomalies as leading drivers of water levels in the Salish Sea (Soontiens et al., 2016; Yang et al., 2019; Grossman et al., 2023).

The wave climate in the Salish Sea is complex, representing the combined influence of swell and locally generated seas. The Strait of Juan de Fuca connects to the open ocean, allowing swell penetration from the relatively intense wave climate of the northeast Pacific Ocean. Winter mean wave height for the northeast Pacific is 3.8 m, with winter storms often producing wave heights greater than 10 m (Ruggiero et al., 2010). These winter swells are primarily from the west – northwest (Stevens et al., 2024), allowing direct propagation into the strait. Past the strait of Juan de Fuca, the Salish Sea wave climate is confined to local seas, but with wave characteristics strongly dependent on location due to rapidly varying fetch and wind characteristics derived from complex topography.

https://doi.org/10.5194/egusphere-2026-3369
Preprint. Discussion started: 22 July 2026

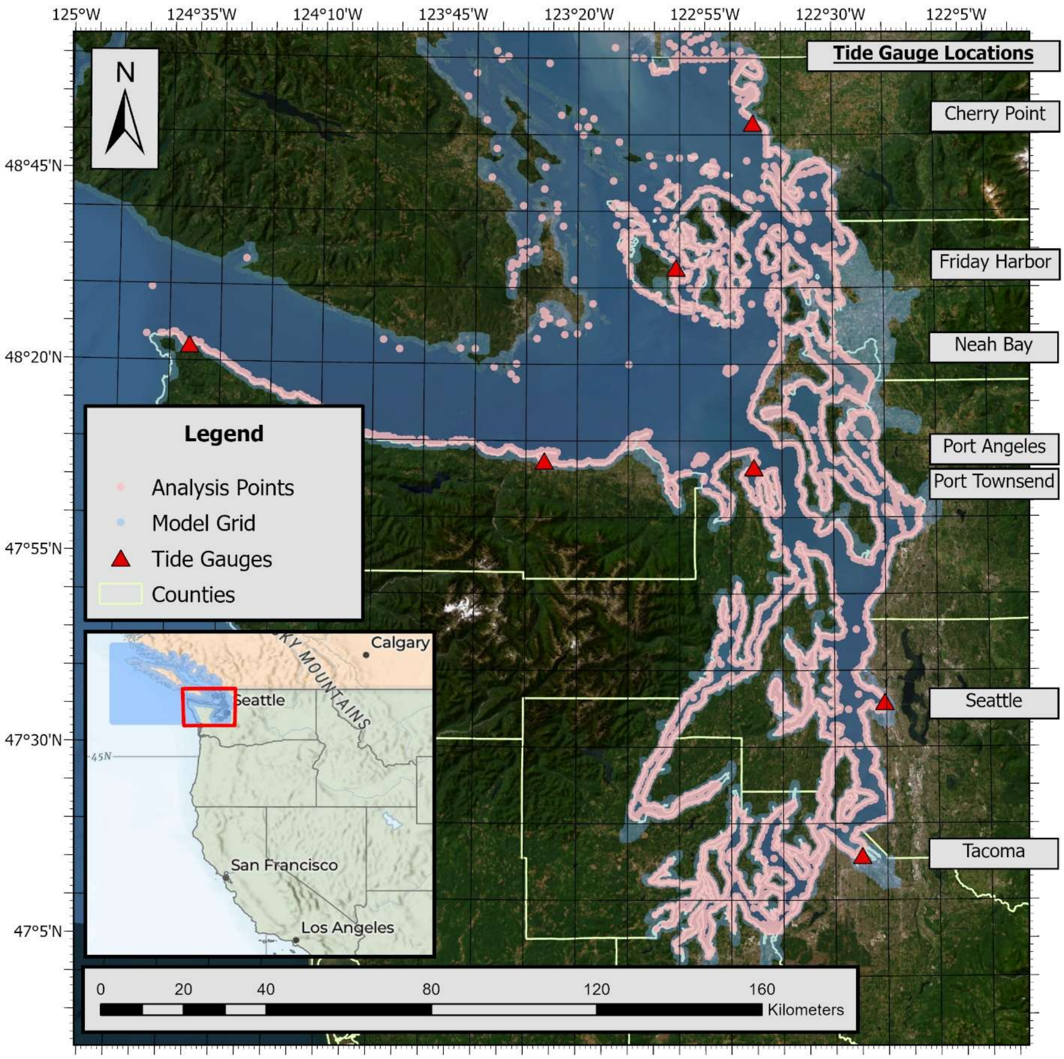

130 **Figure 1: Study Site: Salish Sea, Washington, USA. Analysis stations (both water levels and waves) are plotted as pink points and concentrated on the U.S. portion of the region. The hydrodynamic model grid extent is shaded blue in the inset figure, and tide gauges are marked as red triangles (see table A1 for tide gauge information). Basemap credit: Earthstar Geographics, Esri | Powered by Esri.**

https://doi.org/10.5194/egusphere-2026-3369
Preprint. Discussion started: 22 July 2026

2.2 Input Data

This study utilizes a variety of input datasets to both build and validate models of the system as well as force the models under different climate scenarios. All datasets used for building and validating models are discussed in the Methods section (section 3) under the specific model subsection (for example, 3.1 Wave Model). Two types of input climate data were utilized for forcing: reanalysis data (refer to section 2.2.1 ERA5) and climate model data (both historical and future periods, refer to section 2.2.2 CMIP6). SLR also represents a key driver of coastal hazards and is discussed in section 2.2.3.

2.2.1 ERA5 (Reanalysis Data)

ERA5 (fifth generation ECMWF atmospheric reanalysis of the global climate; Hersbach et al., 2023) reanalysis wind, atmospheric pressure, and wave forcing fields were used to simulate the hindcast period. ERA5 is a global product but features relatively high temporal (hourly) and spatial (31-km grid) resolution. Validations of ERA5 have shown strong model skill, with significant gains over previous global scale products due to increased data assimilation and improved model physics and resolution (Haiden et al., 2019; Rivas and Stoffelen, 2019). An additional strength of the ERA5 reanalysis is a long record length (1940 to near present) due to the recent ERA5 extension (Soci et al., 2024). Long record lengths are important for characterizing extremes, especially in mesotidal environments. An analysis by Abeysirigunawardena et al. (2011) using a 57-year hourly timeseries found that only 5% of the highest surge events in the Salish Sea's Canadian waters occurred during high tides. Therefore, a robust characterization of extreme risk in the region necessitates the longest record lengths possible to fully explore the unlikely co-occurrence of a high tide and high surge events.

This study utilized data for the period 1940–2023 for reanalysis simulations of water levels and waves. ERA5 surface wind and pressure fields were extracted for the entire study region, as well as ERA5 bulk wave parameters (Komen et al., 1994) at the entrance to the Strait of Juan de Fuca. ERA5 wave data were used as a swell component entering the Strait and were chosen for consistency with the atmospheric forcing. Additionally, the ERA5 wave reanalysis has been shown to perform well against other global scale wave products (Timmermans et al., 2020).

https://doi.org/10.5194/egusphere-2026-3369
Preprint. Discussion started: 22 July 2026

2.2.2 CMIP6 (Climate Model Data)

CMIP6 (Eyring et al., 2016) represents the most recent iteration of the Climate Model Intercomparison Project (CMIP). CMIP6 involved a significant restructuring in comparison to previous CMIP versions, allowing for more flexibility in experiments (Model Intercomparison Projects or MIPs) while also providing long-term continuity. This study utilizes a subset of the overall CMIP6 project, the High-Resolution Model Intercomparison Project (HighResMIP) (Haarsma et al., 2016) which focuses on high resolution (25-50 km atmosphere resolution and 10-25 km ocean resolution) GCM simulations. The HighResMIP simulations span the period 1950–2050 and thus have a shorter record length than the standard CMIP6 model implementations (typically 1850 – 2100). This shorter record length represents a compromise due to the higher computational cost of increased resolution. HighResMIP was chosen due to the importance of high resolution forcing for ocean and atmospheric modeling. Multiple studies have shown the importance of high-resolution wind fields in wave modeling (Cavaleri and Bertotti, 2006; Crosby et al., 2023); therefore, utilization of the highest possible resolution GCM was prioritized. Furthermore, increased resolution is necessary for reproducing storm structure, such as in tropical cyclones and extra-tropical storms (Gao et al., 2019; Roberts et al., 2019).

Even with recent improvements to physics and resolution, GCMs are unable (nor intended) to reproduce observed weather events or their exact time series. Reasons for this range from the chaotic nature of weather to modeling limitations (e.g., resolution, unresolved physics). GCMs instead represent the statistical characteristics of climate, with outputs considered plausible stochastic iterations. An ensemble is commonly used for analysis to reduce uncertainty in GCM predictions and provide robustness through averaging across multiple members. This study follows this best practice methodology and utilizes an ensemble of 7 GCM outputs. As for the initiation of this study, the HighResMIP project was still in progress, and data were only available for a subset of the overall ensemble. The 7 models chosen were based on availability as well as alignment with the GTSMip project (Muis et al., 2023) (refer to Table 1).

https://doi.org/10.5194/egusphere-2026-3369
Preprint. Discussion started: 22 July 2026

Table 1: Specific HighResMIP ensemble iterations used in this study.

GCM	- Variant	- Historical Span (Years)	- Future Span (Years)	Model Resolution Atm. (km)	Ocean (km)	Output (Hour)
HadGEM3-GC31-HM-highres-future	r1i1p1f1	1951-2015	2016-2051	50	25	3
HadGEM_GC31_HH_highres-future	r1i1p1f1_gn	1950-2015	2015-2051	50	10	3
HadGEM3-GC31-HM_highresSST-future	r1i1p1f1_gn	1950-2015	2015-2051	50	25	3
EC-Earth3P-HR	r1i1p1f1_gr	1950-2015	2015-2051	50	25	3
CMCC-CM2-VHR4	r1i1p1f1_gn	1950-2015	2015-2051	25	25	6
CNRM-CM6-1-HR	r1i1p1f2_gr	1950-2015	2015-2050	100	25	3
GFDL-CM4C192-highresSST	r1i1p1f1_gr3	1951-2015	2016-2051	50	25	3

All models were run for both a historical and future CMIP6 period. This paired framework allows for a measurement of change that is independent of the individual biases in each CMIP6 climate model. Historical period results are modeled with observed carbon emissions and climate forcing. Future projections, used for this study, are based on the Shared Socioeconomic Pathway 5-8.5 (SSP5-8.5, similar to the RCP8.5 scenario). SSP5-8.5 represents a "business as usual" scenario in which substantial reductions in carbon emissions do not occur until after 2050, the end-period in this study. That said, a significant deviation in ocean-related processes due to different SSP trajectories is not likely to occur until post 2050, after which different SSP trajectories diverge and increase in rate of change. While SSP trajectories remain similar up to 2050, major differences in ocean-related processes are evident compared to simple linear extrapolations from observations. This means that modeled hazards, up to 2050, would

https://doi.org/10.5194/egusphere-2026-3369
Preprint. Discussion started: 22 July 2026

likely be similar even under a lower emissions pathway, although still different from a stationary or extrapolation-based analysis.

All references to CMIP6 or the CMIP6 ensemble in this paper are in reference to the HighResMIP project and its data for the Salish Sea region.

2.2.3 Sea Level Rise (SLR)

The overall modeling framework (both the wave and hydrodynamic models) were run for the following set of SLR scenarios of 0, 0.25, 0.50, 1.0, 1.5, 2.0, and 3.0 meters, consistent with the U.S. Geological Survey (USGS) Coastal Storm Modeling System project (CoSMoS; Barnard et al., 2014, Barnard et al., 2024) and more recent federal SLR guidance (Sweet et al., 2022). SLR is treated in a "stationary" manner and is included as a bulk increase to mean sea level in the Pacific Ocean that does not vary temporally or spatially within the Salish Sea. This approach allows users to choose a SLR scenario that matches their level of flood risk tolerance and then relate the outputs to planning time horizons based on the best available SLR projections for their region. Relative SLR trajectories are spatially variable and updated periodically with improving science. Additionally, SLR projections include considerable uncertainty due to both modeling limitations and uncertainty in future greenhouse gas emissions. By taking a time-independent approach of sampling across plausible SLR positions, the output products are not tied to a specific SLR trajectory through time and can continue to be used as local projections are refined and updated. Work by Miller et al. (2018) details current regional projections for SLR across coastal Washington. Example relative SLR projections for 2100 in the Salish Sea region range from 2.5 m (Tacoma, where land subsidence occurs, High Greenhouse Gas Scenario, Median estimate) to 0.5 m (Neah Bay, where land is uplifting, Low Greenhouse Gas Scenario, Median estimate).

An additional outcome of this approach is that modeled changes (as controlled both by SLR and changing climatic conditions) are considered as the difference between two stationary periods. This simplifies comparison and allows a larger sample in computing the difference. Specifically, water levels and wave energy have significant long-term patterns, so a long record is necessary to robustly compute change

https://doi.org/10.5194/egusphere-2026-3369
Preprint. Discussion started: 22 July 2026

outside of natural variability. For example, an anomalously energetic storm season, such as a single winter characterized by multiple extreme wave events, may produce elevated wave energy over several months, yet this signal does not necessarily indicate a persistent trend in wave heights. To robustly sample change, we characterize change as the difference between two stationary climatologies, each spanning 30 years, consistent with World Meteorological Organization (WMO) climatological normals (World Meteorological Organization, 2017). This approach reduces the influence of short-term variability and episodic extremes while more effectively capturing underlying decadal-scale climate variability.

3. Methods

3.1 Wave Model

Waves are important contributors to coastal water levels, with wave setup and swash contributing significantly to coastal hazards (Barnard et al., 2014; Idier et al., 2019; Erikson et al., 2018). The Salish Sea presents a unique challenge for wave modeling, with complex shorelines, bathymetry, and localized wind effects.

This study builds on a computationally efficient approach to rapidly model regional wave characteristics combining outputs from a comprehensive set of look-up tables created with the Simulating WAves Nearshore (SWAN; Booij et al., 1999) model and linear swell propagation for all potential conditions (Crosby et al., 2023). The model was run with stationary conditions and time-varying water levels produced by the hydrodynamic model (refer to section 3.2). The utilized hybrid modeling approach (statistical/dynamic modeling framework) was chosen because it facilitates rapid simulation of long periods across large spatial scales while achieving skill comparable to standard SWAN implementations (Crosby et al., 2023).

Differences from Crosby et al. (2023) include 1) switching meteorological forcing from the High-Resolution Deterministic Prediction System (HRDPS) produced by Environment and Climate Change Canada (Environment and Climate Change Canada, 2024).

https://doi.org/10.5194/egusphere-2026-3369
Preprint. Discussion started: 22 July 2026

to ERA5 and 2) application of the modeling approach to CMIP6 forcing. The switch to ERA5 was made for two reasons. First, the switch allowed us to leverage the much larger record length of the ERA5 time series. A long record length is critical for capturing extremes and for characterizing a climatology that is free of shorter period variability. Second, this study primarily focuses on climate-driven changes to waves and water levels as predicted by CMIP6. Wave model fidelity is strongly controlled by wind resolution (Yang et al., 2019), and the model resolution of the CMIP6 ensemble is closer to ERA5 than to HRDPS. Using a much higher resolution meteorological source for validation could present a false sense of model skill that is not shared by the CMIP6 forced versions of the model. This study is primarily concerned with modeling future changes to forcing and it is assumed, as is often the case in the climate modeling context, that the measured change from the historical to future period is still valid even if the model itself is biased.

In general, lower resolution wind products exhibit bias in magnitude as compared to higher resolution products, especially for extremes (Solbrekke et al., 2021). A similar trend was found for the Salish Sea when comparing ERA5 winds to observed data, although a comprehensive analysis was limited by sparse wind data across the region. To compensate for biases and limited observational data, ERA5 winds were bias corrected using the higher resolution HRDPS dataset as a target. At each wave output station, winds were extracted from both nearest ERA5 and HRDPS grid points. The full ERA5 timeseries was then bias corrected using quantile mapping (as detailed in Parker and Hill, 2017) to match the cumulative distribution function (CDF) of the HRDPS data. For the case of the future CMIP6 dataset, Equidistant Quantile Matching was used to preserve the change signal between the CMIP6 historic and future periods (refer to Parker and Hill, 2017 for details).

3.2 Hydrodynamic Model

Hydrodynamic modeling was performed at the regional scale (full Salish Sea) using Delft3D Flexible Mesh (Delft3D FM, Kernkamp, 2011, Figure 1). The utilized model is fully described and validated in Grossman et al. (2023) and is briefly summarized here. Delft3D FM uses an unstructured mesh to solve the shallow water equations, in this implementation using the 2D depth-averaged mode. The model domain covers the full Salish Sea (Figure 1), with the offshore model boundary located approximately

180 km offshore of the entrance to the Strait of Juan de Fuca. Model resolution varies from ~1 km for the offshore extent to ~150 m for nearshore coastal areas. Output stations are concentrated along the U.S. coastline in the nearshore. Overall, the model was found to demonstrate high skill in reproducing still water levels (SWL), with a mean root mean square error (RMSE) of approximately 10 cm across six National Oceanic and Atmospheric Administration (NOAA) tide stations and seven USGS water level gauges during the validation period from 2017 to 2019 (Grossman et al., 2023).

The offshore boundary of the model was forced with tidal constituents and sea level anomalies (e.g., El Niño, coastal upwelling) Tidal forcing was provided by the FES2014 model (Lyard, 2021). Here, sea level anomalies were modeled using the same framework as detailed in Grossman et al. (2023) but with regression coefficients calibrated for ERA5 forcing. As an additional change to the model implementation described in Grossman et al., (2023), the model was forced with wind and pressure fields derived from the CMIP6 model ensemble and the ERA5 reanalysis. These products are detailed in sections 2.2.1 (ERA5) and 2.2.2 (CMIP6), while the specific simulation periods are detailed in 3.3 (Simulation Periods).

3.3 Simulation Periods and Analysis

The wave and hydrodynamic models detailed above were run for 3 periods: Reanalysis, CMIP6 historic, and CMIP6 future. Despite being computationally intensive, this structure was chosen to provide information both for model validation (Reanalysis period) and measured change (CMIP6 historic and future). Details of the models and their simulation periods are listed in Table 2. Of note, the conversion of calendar year data to water year resulted in a slightly smaller run span than the full available data (e.g., 1940 was not run because the 1940 water year would require data from 1939). In addition to the ensemble of runs listed in Table 2, the CMIP6 future simulations were run at a set of SLR scenarios (refer to section 2.2.3 Sea Level Rise).

Table 2: Simulation Periods

https://doi.org/10.5194/egusphere-2026-3369
Preprint. Discussion started: 22 July 2026

Name	Model	Ensemble Members	Span (Years)	SLR Scenarios (cm)
Reanalysis	ERA5	1	1941-2023	0
Historical	CMIP6 Historical	7	~1950-2015	0
Future	CMIP6 Future	7	~2015-2051	0, 25, 50, 100, 150, 200, 300

The above detailed modeling framework produced a large amount of data (>30 TB) with a high level of dimensionality (e.g., multiple SLR scenarios, output stations, climate models, decades). Of this large dataset, this study focuses on changes in the future and extremes. Extremes are considered using empirical return intervals based on the Weibull plotting position (P = m / (n+1) where m is rank and n is sample size). This approach avoids convolving physical modeling results with extreme value distribution fitting, acknowledging that extremes can be sensitive to the specific implementation of an extreme value model. The Weibull plotting position is unbiased for ranked data and is standard practice for hydrologic extremes (Makkonen, 2006). The choice of using empirical return intervals constrains the maximum return period event by the length of the climatological period (~30 years for this study). Differences in extremes are determined by calculating the corresponding return period value, using the empirical definition, for the future and historical periods. The change is then calculated by subtracting the historical values from the future values.

Additionally, results are split by basin for some of the analysis to reduce the dimensionality of the data and assist in interpretation. The distribution of the basins is detailed in Figure 2 and approximately follows the delineation proposed in Walker et al., (2022).

https://doi.org/10.5194/egusphere-2026-3369
Preprint. Discussion started: 22 July 2026

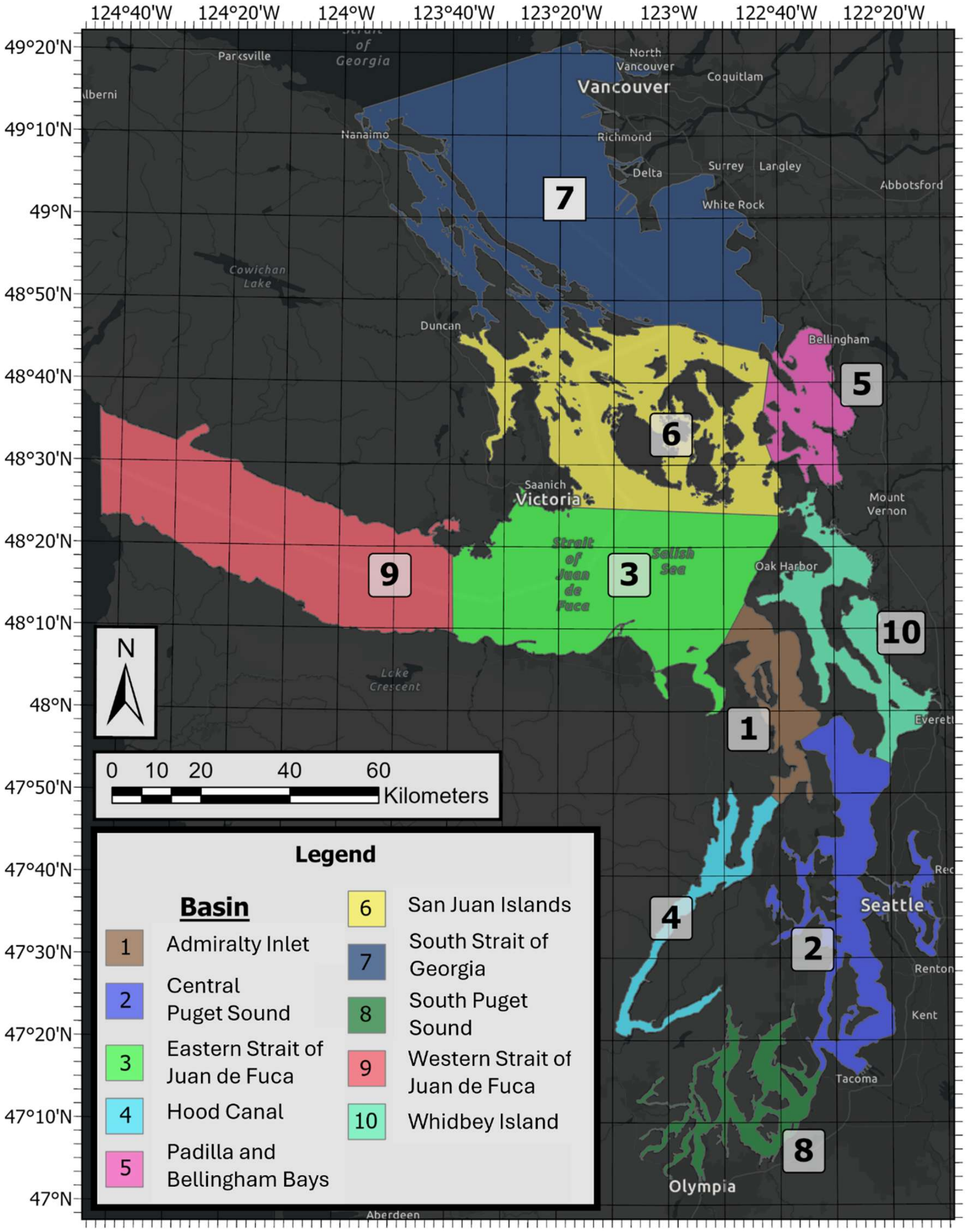

Figure 2: General Schematization of basins of the Salish Sea. Basins are used for spatial aggregation of results. Basemap credit: Esri, TomTom, Garmin, FAO, NOAA, USGS, © OpenStreetMap contributors, and the GIS User Community | powered by Esri.

https://doi.org/10.5194/egusphere-2026-3369
Preprint. Discussion started: 22 July 2026

4. Model-Observation Comparisons

A full exploration of wave model performance is provided in Crosby et al. (2023), and a full exploration of hydrodynamic model performance is provided in Grossman et al. (2023). Atmospheric forcing was updated for this study, so a brief explanation of how model performance has changed is detailed here. Additional information is available in Appendix A: Model Validation.

The NOAA tide gauge database (Center for Operational Oceanographic Products and Services, 2022) was used to validate the utilized water level modeling framework. The Salish Sea is sampled by 7 tide gauges, many with long-term data records. The full available 6-min observed water-level intervals were used (Fig. 1) from NOAA gauges 9443090, 9444090, 9444900, 9447230, 9446484, 9449880, 9449424. The overall RMSE of 14 cm is comparable to other regional scale modeling efforts in similar systems. For example, Olabarrieta et al. (2011) showed an RMSE of ~16 cm using a physically complex 3-D coupled hydrodynamic/wave model. RMSE of modeled water levels were found to increase by an average of 3 cm across all gauges for the model implementation described here using ERA5 forcing as compared to the model forced with higher resolution data (as in Grossman et al., (2023)). This small decrease in performance was deemed acceptable for the added gain of a significantly longer record length.

For waves, a comparison of significant wave heights across all wave buoys (National Data Buoy Center, 2022) and observational deployments (Grossman et al., 2024, Nowacki et al., 2023, Crosby and Grossman, 2019) locations showed an average RMSE of 20 cm. This RMSE is consistent with the performance reported for the model forced with higher-resolution winds in Crosby et al. (2023), which showed an average RMSE of 21 cm. Wave periods were not explored in this paper but showed an increase in RMSE from 1.12 seconds to 1.29 seconds by using the coarser resolution ERA5 winds. This relatively consistent model performance across model implementations does not contradict the well-established fact that wind resolution is important for waves but rather implies that the utilized bias correction of winds is compensating well for the resolution deficiency.

https://doi.org/10.5194/egusphere-2026-3369
Preprint. Discussion started: 22 July 2026

5. Results

5.1 Climate-induced changes to extreme water levels and waves

Model results for specific locations and SLR scenarios provide an initial visualization of changes in water levels, waves, and ensemble variability before evaluating more complex spatial results and relative contributions of forcings. Figure 3 plots return interval curves, for water levels and significant wave height at Seattle and Friday Harbor, two locations that represent dynamically different regions of the Salish Sea. Seattle is within the central Puget Sound Basin, with larger tides and smaller fetch limited waves, while Friday Harbor is located within the San Juan Islands Basin and is more exposed to storms and swell down the Strait of Juan de Fuca. The CMIP6 models and ensemble average represent the future period and are plotted for the 0 cm SLR scenario to highlight changes into the future only from changes to forcing. The difference between the return intervals for the reanalysis period (black) and CMIP6 future period (blue) represents the predicted change in extremes at the corresponding return period (x-axis). Also plotted are the return interval curves for each individual CMIP6 model (dotted colored lines) to show spread across the CMIP6 models. To further quantify uncertainty, the 95% confidence interval was calculated using a one-sample confidence interval for the mean with the sample being the CMIP6 model values at each return period. This 95% confidence interval is plotted as a grey region and quantifies the spread of the ensemble but does not capture increasing statistical uncertainty when moving to more extreme events.

https://doi.org/10.5194/egusphere-2026-3369
Preprint. Discussion started: 22 July 2026

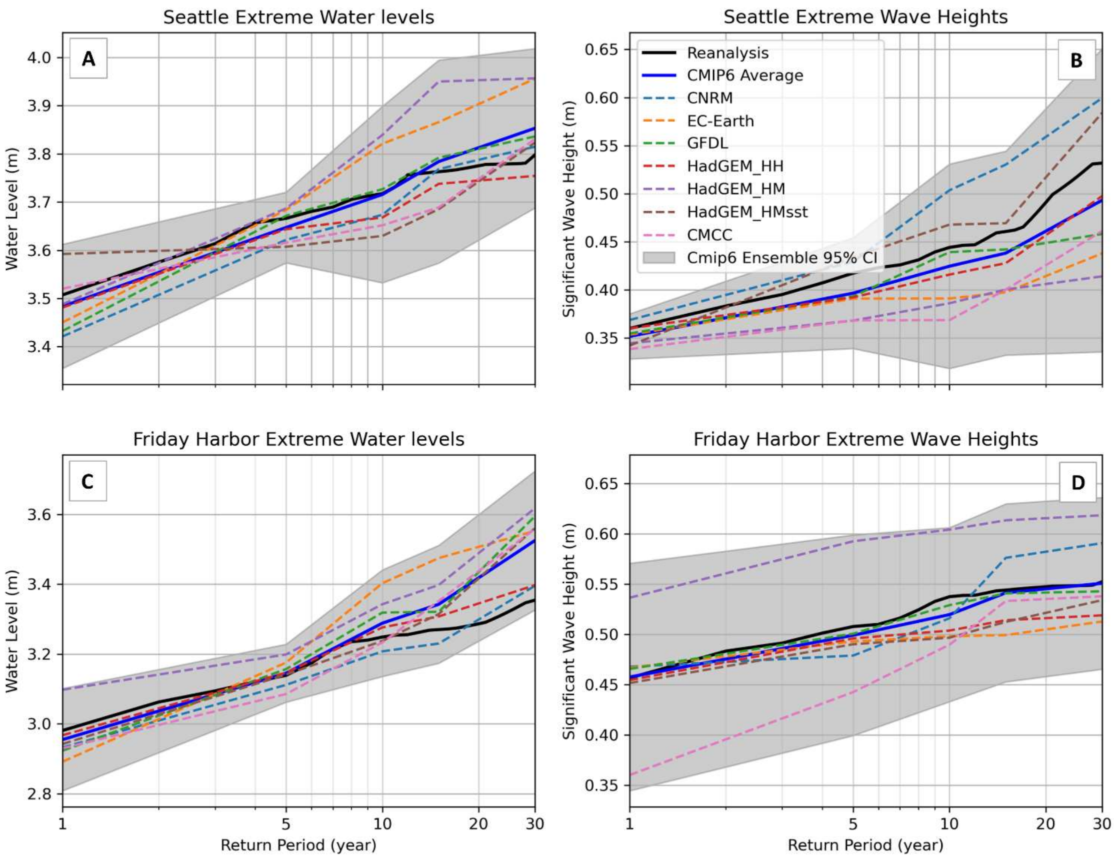

Figure 3: Return interval curves for water levels (meters NAVD88: subplot A, C) and waves (meters significant wave height: subplot B, D) at two locations, Seattle (NOAA Gauge 9447130: subplot A, B) and Friday Harbor (NOAA Gauge 9449880: subplot C, D) for the current sea level state. Return interval curves are plotted for the ERA5 Reanalysis (black) and CMIP6 future (average across ensemble: dark blue) period. Individual CMIP6 models are plotted as colored dotted lines, and the 95% confidence interval (based on CMIP6 samples) is plotted as a grey patch.

The first notable result in Figure 3 is that the modeled climate-driven change varies across return periods. This is evident in the differing offsets between reanalysis water levels (bold black) and future projections (blue lines) as return periods increase. For water levels, measured change is negative (a predicted decrease) for low return period events (e.g., annual) but positive (a predicted increase) for higher return periods (e.g., the 30-year event). For wave heights, the Seattle location shows a general decrease across

https://doi.org/10.5194/egusphere-2026-3369
Preprint. Discussion started: 22 July 2026

extremes while minimal change is predicted for the Friday Harbor location. This variability in extreme value space complicates integrated hazard assessments because different quantiles exhibit changes in opposite directions.

A key caveat to this conclusion, and a second major result from Figure 3, is that modeled changes are small compared to uncertainty. Predicted change does not exceed the 95% uncertainty limits for any presented stations or variables. Although measurable changes are present and reach up to a 20 cm increase in water levels at Friday Harbor for the 30-yr return period, the spread among CMIP6 models is sufficiently large that these changes are not statistically distinguishable from zero. This indicates that inter-model disagreement currently exceeds any detectable climate-forced signal for the 2050 horizon. The largest projected changes occur at higher return periods, but these are also the points of greatest uncertainty, both in the model ensemble and in empirical estimates, because the 30-year event is represented by only a single sample in the observational record.

5.2 Changes as a function of space

Figure 3 illustrates results at only two locations, raising the question of whether these results are more generally applicable across the Salish Sea. Figure 4 addresses this by mapping modeled changes to the annual and 30-year return period (RP) water level and significant wave height as averaged across the CMIP6 ensemble. Results are examined for the present SLR position (refer to section 5.5 for an analysis of SLR effects). Overall results show that a general decrease is predicted for annual water levels across the Salish Sea. Conversely, 30-year RP water levels are expected to increase broadly, meaning that regional trends follow the results shown in Figure 3. Waves are predicted to have more spatial variability, with some locations showing increases and other decreases. In general, the southern basins (south Puget Sound, central Puget Sound, and Hood Canal Basins) show a general decrease in waves that transition to a less spatially consistent change (more local variability) in the northern basins. Local variability is likely due to changes in wind direction and local coastline alignment affecting fetch and local impacts. Changes in water level are generally greater, reaching up to around 20 cm, while wave changes are smaller (less

https://doi.org/10.5194/egusphere-2026-3369
Preprint. Discussion started: 22 July 2026

than 10 cm). However, because waves in the Puget Sound are generally less than 2 m in the Strait of Juan de Fuca basins and less than 1 m elsewhere, the percentage change in wave height is comparable in scale to that of water levels.

https://doi.org/10.5194/egusphere-2026-3369
Preprint. Discussion started: 22 July 2026

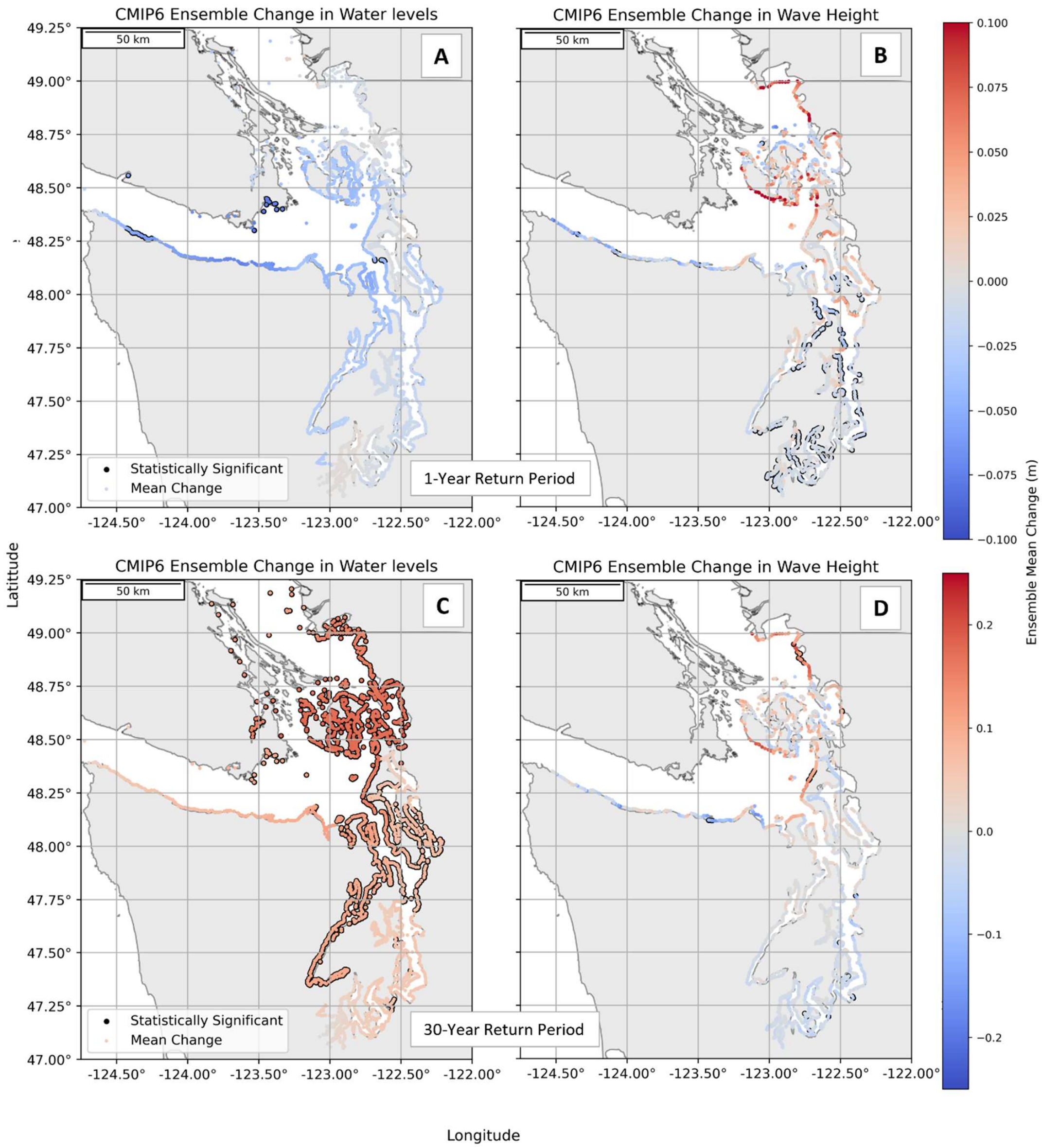

415 **Figure 4: Changes to the annual (subplot A, B) and 30-year (subplot C, D) return interval water levels (subplot A, C) and significant wave heights (subplot B, D). Plotted changes are the mean of the CMIP6 ensemble with color bars representing the whole row (e.g., both subplot A and B). Statistically significant (p-value < 0.05) changes are marked with a black outline. Land is plotted as a grey region (shapefile by ESRI | Powered by Esri).**

https://doi.org/10.5194/egusphere-2026-3369
Preprint. Discussion started: 22 July 2026

As shown in Figure 3, a strength of the utilized methodology is that the ensemble provides information on the significance of the measured change. For Figure 4, a one-sample t-test is used to test if the measured change is significant at the 95% confidence level (mean difference is different than zero) and plotted by highlighting statistically significant stations with a dark outline (all stations with a p-value < 0.05). Overall, this plot confirms earlier results that much of the Salish Sea does not show statistically significant changes to waves or water levels; 30-year water levels are the exception within some basins: Hood Canal, Admiralty Inlet, San Juan Islands, Padilla and Bellingham Bays, and some of central Puget Sound. Changes to waves are generally not found significant, except for scattered segments for the annual return period mostly concentrated towards the southern basins of Puget Sound and segments along the Straight of San Juan de Fuca south coasts.

5.3 Changes as a function of return period

We addressed whether modeled changes to water levels and waves are uniform across return periods (plotted in Figure 4 are only the annual and 30-year return periods). To explore this dimension of the data, a subset of return periods (annual, 5-year, 10-year, 15-year, and 30-year) are plotted in Figure 5, aggregated at each of the basins detailed in Figure 2. Variability across stations in each basin and across the CMIP6 ensemble is included within the violin plot density estimates (shading behind bars, Fig. 5).

https://doi.org/10.5194/egusphere-2026-3369
Preprint. Discussion started: 22 July 2026

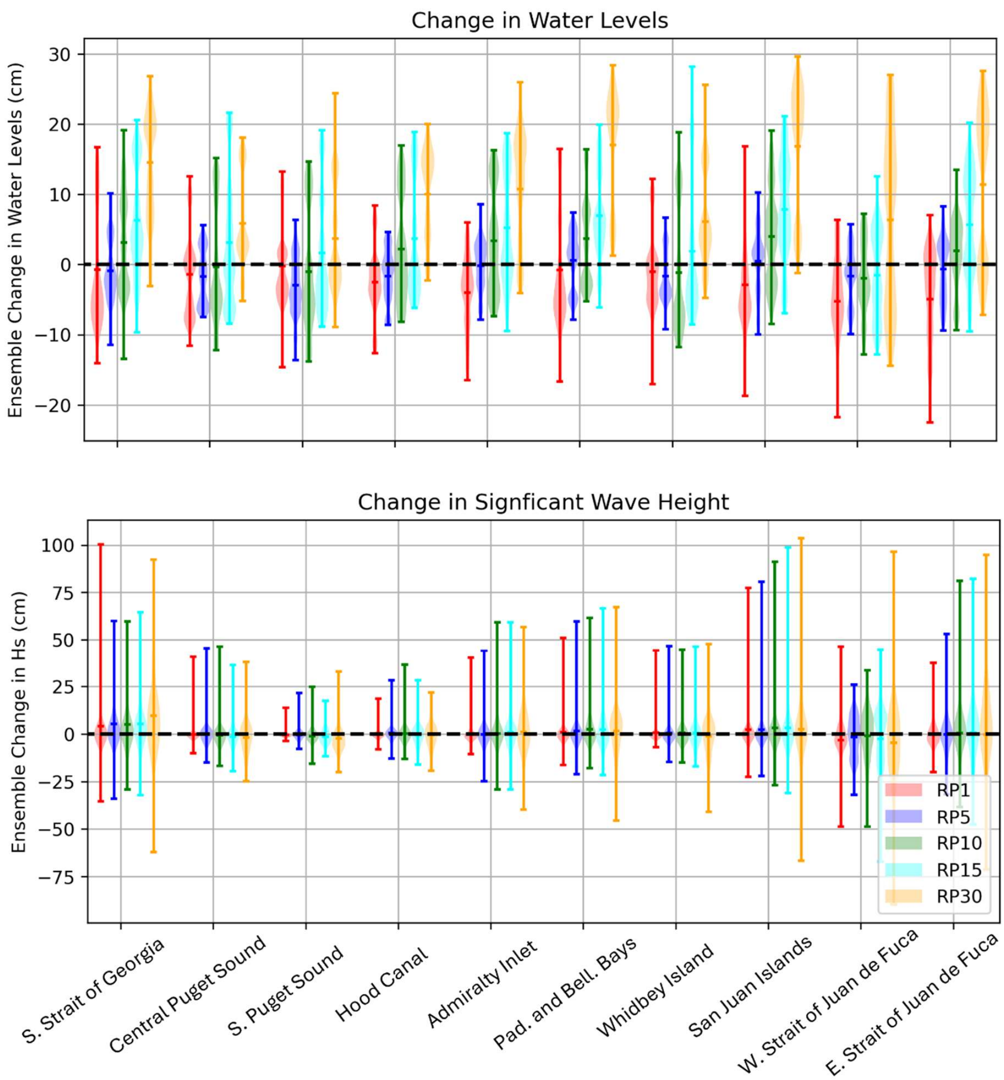

435

Figure 5: Ensemble change in water levels and wave heights for extreme events (Return Period 1 – 30). Changes are aggregated across all members of the CMIP6 ensemble and for all stations in each basin. The variability across this aggregated sample is plotted as density (width of the violin plot) and with the mean and min/max extremes plotted as vertical lines.

https://doi.org/10.5194/egusphere-2026-3369
Preprint. Discussion started: 22 July 2026

Figure 5, subplot A, shows a distinct trend in how water levels are projected to change as a function of return period. Specifically, this plot reaffirms results shown in Figure 3, that water level change increases with higher return period in each basin. For all basins, the annual (RP 1) shows a decrease in water levels into the future (although small and not statistically significant) but increases (up to nearly 20 cm of increase) for the 30-year event.

Significant wave height change (Figure 5B) is less consistent across return periods. Although subtle due to the plot scale, the ensemble mean predictions indicate both increases and decreases in wave heights with increasing return period, depending on the basin. Notably the y-axis range for significant wave height changes is an order of magnitude larger than that for water level changes, reflecting greater variability in the wave response. This uncertainty primarily is sourced from the CMIP6 wind forcing, with significant disagreement across the ensemble, both in terms of magnitude and sign, for projected changes in wind forcing. There is local variability across basins (refer to Figure 4), but the large range in predicted changes (vertical brackets in the violin plots), is driven by individual CMIP6 model iterations showing very different future wave characteristics. The bulk of predictions (visible by width in the violin plots), is concentrated at smaller changes with outliers driving the width of the violin plot bars. Overall, this result (uncertainty and local variability strongly controlling CMIP6 predicted changes) complicates efforts to make basin-scale general conclusions regarding changes to wave height.

Figure 5 shows that for both significant wave height and water levels, projected future changes exhibit substantial variability, as indicated by the density distributions and whiskers in the violin plots. This variability combines spatial inhomogeneity across the basins and across the CMIP6 ensemble. Therefore, the overall large spread in the data emphasizes the need for both an ensemble of climate models and spatially explicit data. A lack of either of these components would give unrealistic impressions of the uncertainty in the data and a less robust answer (for example if an outlier station or CMIP6 model member was used). This result is especially true for waves where variability in predicted change is an order of magnitude greater than the mean change signal itself. Results in Figure 3 illustrate the importance of this conclusion, where for Friday Harbor extreme waves, the HadGem-HM model shows the complete

https://doi.org/10.5194/egusphere-2026-3369
Preprint. Discussion started: 22 July 2026

opposite sign, as well as a much greater magnitude, of change compared to other models. Overall, the large variability indicates that changes in extreme water levels and significant wave heights are relatively uncertain across the Salish Sea (also refer to significance testing in Figure 4).

5.4 Changes as a function of Season

To further decompose how changes in water levels are projected into the future, an additional view is presented in Figure 6. In Figure 6, changes in water levels are decomposed by season and plotted by individual climate model. We report changes by season as previous research has highlighted that annual-mean values can mask substantial seasonal shifts under warming conditions. Specifically for hydrology in the Salish Sea Basin, significant seasonal changes manifest as decreasing flows in the summer and increasing flows in the winter (with the mean change averaging out to around zero) (CIG, 2015; Buitink et al., 2025). Finally, Figure 6 shows the individual CMIP6 model deltas, giving insight into the spread between models and showing the individual biases for each ensemble member.

https://doi.org/10.5194/egusphere-2026-3369
Preprint. Discussion started: 22 July 2026

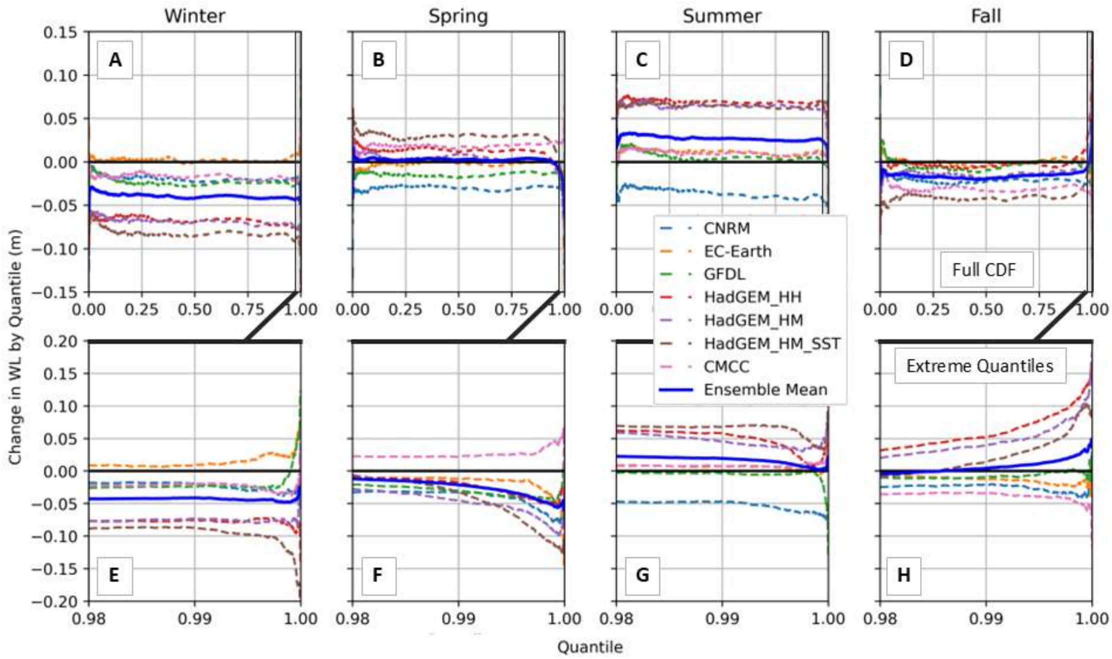

Figure 6: Seasonal variability in changes to water level (WL) by quantile at NOAA tide gauge 9447130 (Seattle). Both the full CDF (subplot A, B, C, D) and a zoom-in on quantiles greater than 0.98 (subplot E, F, G, H) are plotted. Model iterations CNRM (blue), EC-Earth (orange), GFDL (Green), HadGEM-HH (Red), HadGEM-HM (Purple), HadGEM-HM SST (Brown), CMCC (Pink), and the ensemble mean (bold blue) are plotted.

Figure 6 shows that, in general, water levels are expected to decrease slightly in the winter months (December, January, and February) and increase slightly in the summer months (June, July and August). This result is general across the cumulative distribution function (CDF), although behavior can change drastically at the extremes. Even with the x-axis scale change to quantiles greater than 0.98 (Figure 6, subplot E, F, G, and H), extreme behavior (e.g., annual return period events and greater) is not easily visible in this plot because extremes are compressed at approximately the 1.0 quantile (e.g., the 30-year event is approximately the .000099 quantile). Furthermore, general patterns across the CDF start to break down moving towards extremes, with CMIP6 models diverging (Figure 6, subplot E) and signal magnitude changing rapidly (Figure 6, subplot H).

https://doi.org/10.5194/egusphere-2026-3369
Preprint. Discussion started: 22 July 2026

The plotting of individual models further reveals the ensemble spread with some divergent behavior by certain models. For example, CNRM (blue) is substantially lower for a portion of the year (Spring and Summer), and the opposite sign of the ensemble (decrease rather than increase in water levels) for summer. This outlier behaviour brings down the ensemble average for the summer months where other models would predict a larger increase in water levels and erodes the significance of the modeled change. These results emphasize the utility of an ensemble. Figure 6 also shows that changes are potentially larger at the extremes but are also predicted for lower quantiles. While changes to extremes are relevant to coastal hazards, a change to the mean water level can be equally important for coastal dynamics, ecosystems, and many other processes.

5.5 Changes as a function of SLR

The above results focused on changes without considering SLR, and an additional dimension of this dataset couples waves and water levels with sea level scenarios. Recent research has shown the importance of coupled effects of SLR on waves, tides, and non-tidal residual (Idier et al., 2019). However, the magnitude of the nonlinear effects of SLR on waves and water levels is locationally variable and of differing significance, demonstrating its importance as a research topic. Figure 7 examines the nonlinear effect of SLR on changes to water levels by plotting changes at a variety of SLR scenarios (0-3 m of SLR) for each of the basins. Only the nonlinear effect is plotted (the bulk change in water level from SLR is subtracted) because the SLR signal is significantly larger.

https://doi.org/10.5194/egusphere-2026-3369
Preprint. Discussion started: 22 July 2026

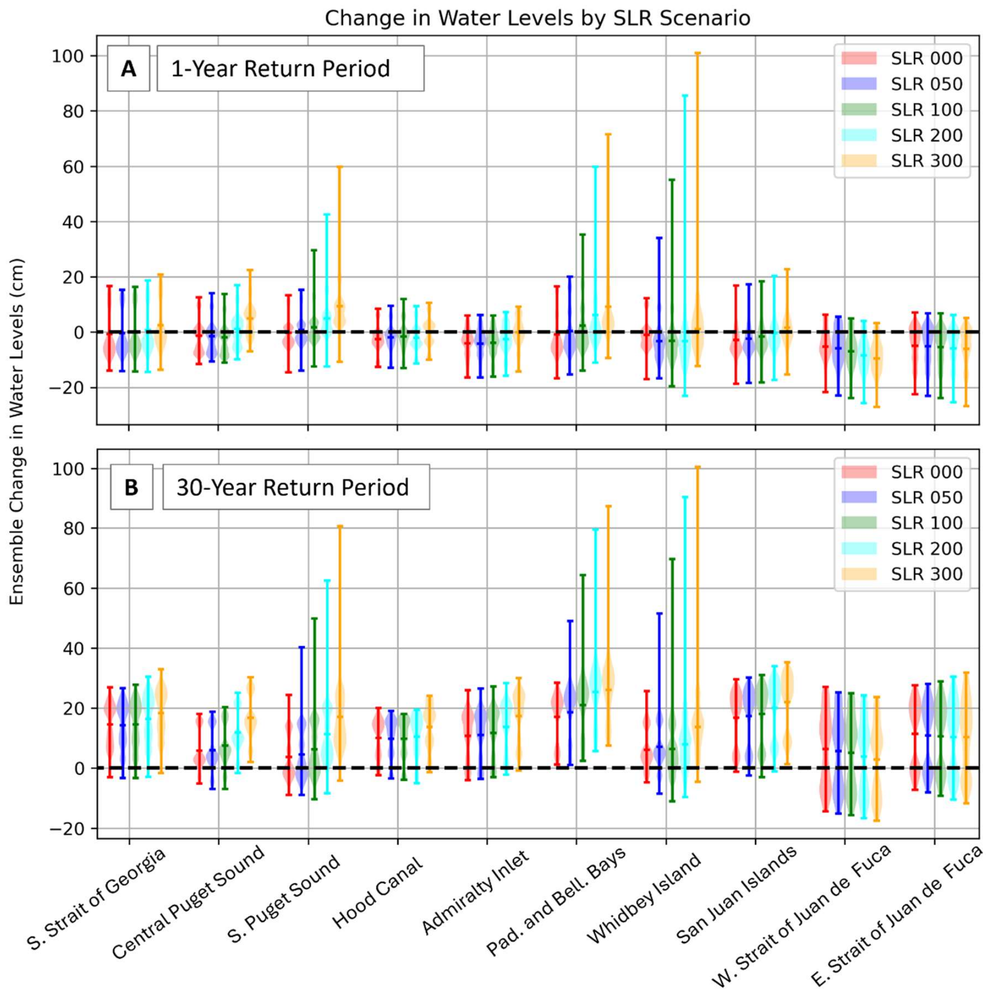

Figure 7: Ensemble change in water levels for the annual (A) and 30-yr (B) event, plotted with increasing sea level rise. Ensemble changes are plotted with SLR removed. Changes are aggregated across the members of the CMIP6 ensemble and for all stations in each basin. The variability across this aggregated sample is plotted as density (width of the violin plot) and with the mean and min/max extremes plotted as horizontal lines.

Figure 7 shows that non-linear effects are present at most basins, shown as a shift in modeled changes to water levels moving from 0 m of SLR to 3 m of SLR. This nonlinear effect can be greater than 10 cm

https://doi.org/10.5194/egusphere-2026-3369
Preprint. Discussion started: 22 July 2026

(e.g., for central Puget Sound or south Puget Sound) or relatively insignificant (e.g., Strait of Juan de Fuca). Both the 1-year event (subplot A) and the 30-year event (subplot B) show a similar pattern but with some differences by basin. For the south Puget Sound, Bellingham Bay and Whidbey Bay Basins, variability greatly increases moving to higher SLR scenarios. This is driven by specific locations in the basins showing larger nonlinear effects, so that while the overall ensemble average may show a modest nonlinear effect, there may be specific locations where the magnitude may be more significant. We hypothesize that for shallow basins further away from the Pacific Ocean, the non-linear effects are largest due to compounding effects and larger change in tidal propagation in shallow water.

6. Discussion

This study introduces a unique dataset, modeling water levels and wave parameters across the Salish Sea for multiple periods (reanalysis, historical, and future CMIP6) and SLR scenarios. This dataset provides a rich characterization of regional coastal dynamics and how they may change into the future. Specifically, continuous and consistent dynamic physical modeling of how coastal storms, waves, and SLR interact provide vital information on long-term spatial and temporal variability. A continuous timeseries approach, while computationally expensive, broadens data usability for downstream work as data is flexibly available across a large spatial and temporal range. This study introduces this dataset, focusing on one aspect (extremes and changes into the future), but acknowledges that this work primarily is a foundation for a wide range of research applications using this base dataset (e.g., Nederhoff et al., 2025).

6.1 Complexity in changes

Results from this study examined how extreme water levels and significant wave heights may change across a variety of dimensions (e.g., space, return period, seasons). A major takeaway from this approach was that, in general, climate-driven changes to water levels cannot be adequately described by a single bulk increase or a uniform adjustment applied across all events. Such an approach can smooth over the underlying physical mechanisms driving change and fail to capture distributional shifts that are not monotonic or uniform. Instead, the modeling framework used here reveals a more complex pattern in which different portions of the water-level distribution change in different directions. For example, the

https://doi.org/10.5194/egusphere-2026-3369
Preprint. Discussion started: 22 July 2026

divergence between annual (decreasing) and 30-year (increasing) return period water level changes shows that climate-forced adjustments can vary substantially across quantiles, emphasizing the importance of explicitly modeling the time series rather than applying a single adjustment factor. In terms of experienced coastal risk, this predicted change signal would manifest as smaller "nuisance-level" flood magnitudes for the most frequent events and increasing magnitudes for the largest, less frequent extremes. From an integrated risk perspective, such as the Expected Annual Flooded Area (EAFA) metric used in Nederhoff et al. (2025), these opposing tendencies may balance each other out, leading to a muted or buffered change in overall risk into the near future even as specific extreme thresholds shift.

The complexity of these patterns is further illustrated through the seasonal and quantile-based analysis shown in Figure 6. Specifically, changes vary seasonally as well as in terms of extremity. This complexity has direct implications for flood-risk assessment and adaptation planning because it demonstrates that the trajectory of future risk depends on bulk changes to extremes and on how those changes are distributed across event magnitudes, seasons, and locations. These results indicate that a method designed to preserve these changes, such as the pseudo-global-warming (PGW) method (Brogli et al., 2023) could be applicable. The PGW strategy consists of applying the climate change signal ("delta") from a global climate model to current atmospheric conditions and running the resulting fields through a high-resolution model. Figure 6 effectively plots the "delta" fields that would be used in a PGW implementation, providing context for how historical flooding may change across the entire distribution of water levels, from common events to the rarest extremes.

6.2 Statistical Uncertainty in Future Changes

As a qualifier to the above conclusions on complexity in changes into the future, most changes were not found to be statistically significant. Climate models have spatially varying levels of agreement across the globe (Tebaldi et al., 2021), and the Salish Sea Basin seems to be a region of less agreement in terms of the near-term future climate. Certain basins exhibit statistically significant change to 30-year water levels, although an analysis based on a longer period could better assess if this extends to higher return periods. An important consideration is that these results are based on a 2050-time horizon. Climate may diverge

https://doi.org/10.5194/egusphere-2026-3369
Preprint. Discussion started: 22 July 2026

further past 2050, and the methodology in this study is unable to qualify longer-term changes (e.g., the often-used 2100-time horizon). While extreme-value analyses using fitted distributions such as generalized Pareto or generalized extreme value models could be used to extrapolate beyond this period, prior studies suggest that increasing non-stationarity, evolving distribution tails, changes in storm regimes, and divergence across emissions scenarios may limit their ability to represent climate behavior after mid-century (e.g., Meehl et al., 2020; Hermans et al., 2024).This is acknowledged as a necessary limitation of the utilized methodology (refer to section 2.2.2). Further work examining changes to 2100 would allow examining higher return period events and whether model consensus on changes to forcing further converges into the future.

A second reason for calculated changes to extremes to be relatively small is the specific mix of forcing for the Salish Sea. Figure 8 shows the water level components across the Salish Sea basins. Here wave height was converted to setup using the common engineering assumption of 20% significant wave height (Vousdoukas et al., 2018). Tide and Non-Tidal Residuals (NTR) were decomposed using a separate model run forced by only tides. Tides are the results from the tides only run, and NTR are the result of subtracting the tides only run from the full forcing run. Results were calculated as the average across extremes determined using a Peak-Over-Threshold methodology. Figure 8 shows that extreme water levels are generally dominated by tides, making up over 70% of the still water level (here defined as tide + Non-Tidal Residual + Wave Setup). Tides are not significantly affected by climate change (although some constituents are atmospherically forced and they are affected by SLR), so the main control on extreme events is approximately static into the future, making measured change small.

https://doi.org/10.5194/egusphere-2026-3369
Preprint. Discussion started: 22 July 2026

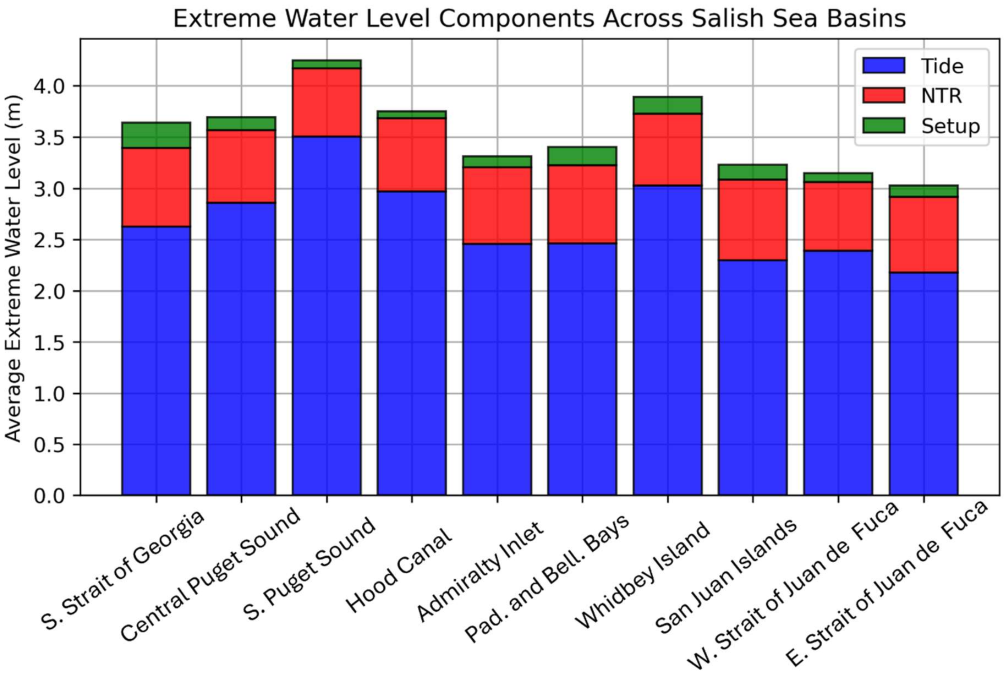

Figure 8: Water level components (tides, non-tidal residual and wave setup) across the Salish Sea for extremes. Magnitude of the bar represents the aggregated average across extremes (determined using Peak-Over-Threshold) and across the basin. Results are for the reanalysis period.

Considering water level extremes from a compound perspective (e.g., waves and water levels combine to drive flooding), the practical significance of changes is further eroded. Due to the dominance of tides, even a large change in significant wave heights would likely not significantly affect flooding in the Salish Sea. Ocean-driven extreme water levels in the Salish Sea are predominantly caused by the occurrence of some forcing (waves or NTR) co-occurring during a large high tide. The forcing on top of high tides is likely not extreme for the individual component because it is highly unlikely that the 30-year significant wave height would co-occur with the 30-year high water level. The unlikely co-occurrence of extremes may define the very extreme tail of possibilities but is not examined here; our analysis is restricted to the 30-year event.

https://doi.org/10.5194/egusphere-2026-3369
Preprint. Discussion started: 22 July 2026

Several studies from other coastal regions show a similar pattern of weak or statistically indistinguishable mid-century changes in atmospheric forcing relevant to waves and storm surge. For example, Muis et al. (2023) found that modeled future changes to storm surge are small compared to uncertainties. Similarly, the IPCC (2023) noted high near-term uncertainty and inter-modal disagreement in climate signals relevant to coastal processes. Collectively, these results emphasize that, for near future to mid-century, the magnitude of modeled changes remains small relative to ensemble spread. While a lack of statistically significant changes may be scientifically "unexciting," it is practically a key result. With large changes in water levels and waves not robustly predicted into the near future, this means that considering current/historical climate as an analogue for the future is a reasonable assumption for much of the Salish Sea. This said, changes may become more significant in the long term (e.g., beyond 2050) and there are locations within the Salish Sea that do have statistically significant signals at higher recurrence intervals (refer to Figure 3).

6.3 Study Limitations

Here, we discuss the limitations of this study to help qualify the interpretations of the results. First, this analysis only considers a subset of the components contributing to flooding. For example, the largest increase in flooding in the Salish Sea Basin may be from fluvial/pluvial changes because precipitation increasingly falls as rain rather than snow during winter months (CIG, 2015). Rain on snow events are often drivers of extreme flooding, and their distribution and frequency may change into the future (Cohen et al., 2015). Additionally, changes to freshwater discharge (both in magnitude and timing) may induce changes to salinity and mixing, potentially affecting density and in turn regional water levels. Finally, anthropogenic changes are a key and highly uncertain contributor to future flood risk, with watershed management, coastal protection, and numerous other factors being first-order controls on experienced coastal risk.

https://doi.org/10.5194/egusphere-2026-3369
Preprint. Discussion started: 22 July 2026

An additional limitation to this study is the coarser resolution of the forcing ERA5 and CMIP6 data. Resolution of wind fields is especially important for wave modeling (Crosby et al., 2023) and the lack of wind downscaling is likely a source of error in the utilized modeling framework. Error from winds is likely concentrated with the wave modeling component because Yang et al., (2019) and Soontiens et al., (2016) found that high-resolution winds did not necessarily improve model performance for surge calculations in the Salish Sea. An alternative strategy could be to downscale CMIP6 atmospheric data to a higher resolution, either using statistical or dynamic downscaling. This would likely improve wave predictions but at a high computational cost. With available resources, downscaling could be done for a single CMIP6 model but not for an ensemble. This study showed that CMIP6 models displayed significant divergent behavior; therefore, running an ensemble as was done in this study is necessary to produce robust future predictions. Figure 6 demonstrates the utility of an ensemble, with the CMIP6 predicted change being of a similar magnitude and opposite sign (e.g., summer and the CNRM or HadGEM-HM models). The arbitrary selection of a single model could therefore have completely changed the calculated delta. This study took the compromise of using lower resolution winds but including more CMIP6 members with the assumption that this will produce a more robust outcome.

Another qualification of this study is that the workflow structure does not give significant power to calculating significance in changes. This study used an ensemble of 7 CMIP6 models, which is significant from a model simulation perspective, but not necessarily for statistical sampling. A sample size of 7 requires large signals to be considered statistically significant at the 95% confidence level. Furthermore, some models were found to exhibit non convergent behaviour (e.g., figure 6, CNRM for summer). While excluding this model could have increased measured change (and significance), exclusion of CMIP6 models should be done with extreme care (Katzenberger et al., 2025). With inter-modal disagreement and relatively subtle changes to processes, measured change was generally found to be insignificant. Running more CMIP6 models to increase the sample size could increase statistical power and buffer outliers but would be computationally prohibitive. An additional possibility would be to explore longer timeframes, e.g., model runs to 2100 where climate change effects may be more robust. At the time of this study, models from the CMIP6 HighResMIP project (used for this study) only extended to 2050. If these models

https://doi.org/10.5194/egusphere-2026-3369
Preprint. Discussion started: 22 July 2026

were extended to 2100, this could provide additional ability to discuss predicted changes to forcing, although at the longer 2100-time horizon rather than 2050.

6.4 Policy Implications

The results of this study have several implications for understanding coastal hazards and for identifying areas where additional scientific investigation may be valuable. A key finding is that climate-driven changes to oceanic forcing (waves, storm surge, wind setup, and non-tidal residuals) are generally small in magnitude and, for most of the region, not statistically significant through 2050. This distinction shapes how these results may be interpreted when considering the allocation of scientific and financial resources. Because modeled changes to waves and water levels fall within the uncertainty range of the CMIP6 ensemble for most basins, present-day storm climatology seems to provide a reasonable analogue for near-future conditions. Under this interpretation, historical extreme events, existing observational datasets, and projected sea-level rise (SLR) could provide a credible basis for hazard assessments.

In contrast to small change signals for forcing, sea level rise (SLR) represents a dominant driver of future coastal hazards. SLR is certainly a contributor to changes in extremes, a result that is not fully highlighted in the above results for which SLR is removed (for plotting non-linear effects, section 5.5) or not considered (0 SLR scenario plotted). As illustrated in Figure 8, SLR rapidly becomes a key factor for extremes in combination with tides because NTR and waves are relatively small. Additionally, SLR is (from an event perspective) temporally constant and so the co-occurrence with a high tide is not necessary for it to contribute to compound extremes. Collectively, these results indicate that SLR is likely to exert a stronger influence on future coastal water levels and shoreline change than projected changes in storminess.

This study additionally examined the non-linear effects of SLR on forcing (refer to section 5.5). Overall non-linear effects were found to be present but were generally not significant. Similar to other findings from this study, capturing these effects is computationally expensive and likely within the uncertainty

https://doi.org/10.5194/egusphere-2026-3369
Preprint. Discussion started: 22 July 2026

bands for predicted future climate. Non-linear effects are small compared to the SLR signal driving the nonlinear effects. For example, the max basin ensemble mean nonlinear change of approximately 10 cm is driven by 300 cm of SLR (and thus is only around 3% of the signal). From a hazards perspective, the SLR signal would dominate the resulting effects. While some locations may exhibit larger nonlinear responses that are averaged out in basin-scale summaries (Figure 7), these can be examined in detail using the full dataset provided.

The modeling workflow used in this study required more than 8,000,000 CPU hours on the USGS High-Performance Computing system. Establishing that climate-forced changes to storminess are unlikely to substantially alter near-term coastal hazards indicates that future scientific assessments may not require similarly intensive modeling to characterize near-future conditions. In such cases, high-resolution topographic and bathymetric data, historical storm climatology, and SLR projections may offer substantial value for understanding exposure. Overall, these findings highlight the relative importance of SLR in shaping near-term coastal hazards in the Salish Sea and help clarify where additional scientific effort may yield the greatest improvements in understanding.

7. Conclusions

This study used a robust ensemble of CMIP6 forced regional models to examine how climate change and SLR are expected to affect waves and water levels in the Salish Sea. Results showed that modeled extreme water levels (e.g., the 30-year event) are expected to increase into the future across the Salish Sea, with the magnitude of change decreasing as events get less extreme and switching to a decrease for annual events. Results for changes to waves are less consistent; waves generally decrease for the southern basins, but the magnitude of the change is not statistically significant. Partitioning results by season show that overall water levels are expected to decrease slightly in the winter months and increase slightly in the summer months.

Using an ensemble allows exploring the significance of measured changes from the larger CMIP6 ensemble. Overall, the CMIP6 ensemble is found to exhibit significant variability for the Salish Sea Basin,

https://doi.org/10.5194/egusphere-2026-3369
Preprint. Discussion started: 22 July 2026

resulting in much of the modeling change to be found not statistically significant. This result highlights the importance of modeling using ensemble methods for analysis because choosing a single CMIP6 ensemble member could result in over 100% differences in calculated change. While using ensemble techniques is computationally costly, the investment is necessary to produce robust estimates of change. The result of non-significant change at the 2050-time horizon is important for forward-looking coastal hazard and coastal processes type analysis because it supports the assumption that present-day conditions are a reasonable proxy for the near future (e.g., 2050). This simplifies analysis and could save considerable effort by removing this source of uncertainty. A key consideration in this outcome is that this study can only examine changes to 2050; therefore, this assumption of non-significance could be incorrect at longer time scales, such as to 2100. Also, improvements to global climate models may increase consensus among climate projections resulting in more significance in forced wave and water level changes.

Finally, this study looked at non-linear effects of SLR on waves and water levels. SLR was found to have some effects on water levels, with the 3 m SLR scenario showing up to 10 cm of additional increase to water levels. While this is numerically significant, important context is that these non-linear effects are in general still small compared to the magnitude of SLR itself. With 3 m of SLR, the difference of 10 cm is likely within flood model uncertainty (and certainly within climate uncertainty) and will be relatively insignificant in terms of impact compared to the much larger SLR signal. Non-linear effects on waves were found to be relatively insignificant, primarily related to the 10-m depth of examined wave output stations.

Overall, this study develops a rich dataset of regional scale water levels and waves as forced by the CMIP6 dataset. **I**n addition to characterizing projected changes in physical drivers across the Salish Sea, the dataset could be used for a range of future scientific analyses related to coastal processes and hazards. For example, the dataset could be applied to local-scale investigations of flood hazard exposure and how such exposure may evolve under different climate trajectories.

https://doi.org/10.5194/egusphere-2026-3369
Preprint. Discussion started: 22 July 2026

Statements and Declarations

Disclaimer:

Any use of trade, firm, or product names is for descriptive purposes only and does not imply endorsement by the U.S. Government.

Copernicus Publications remains neutral with regard to jurisdictional claims made in the text, published maps, institutional affiliations, or any other geographical representation in this paper. While Copernicus Publications makes every effort to include appropriate place names, the final responsibility lies with the authors. Views expressed in the text are those of the authors and do not necessarily reflect the views of the publisher.

Competing interests:

The authors have no competing interests to declare that are relevant to the content of this article.

Financial support

This research was funded by the EPA and the USGS Coastal and Marine Hazards and Resources Program.

Author contributions:

Kai Parker led the analysis and wrote the manuscript with substantive input from all co-authors. Anita Engelstad led the model simulations for the wave component. Kees Nederhoff contributed to overall project coordination and co-developed the overall project workflow. Eric Grossman and Li Erikson contributed to project conceptualization and were responsible for funding acquisition. All authors contributed to the manuscript, reviewed and approved the final manuscript.

Code and data availability:

All data underlying the findings are fully available without restriction from Parker et al., 2026.

Acknowledgments:

We acknowledge the foundational work upon which this work was built, specifically that detailed in Grossman et al., (2023) and Crosby et al., (2023). We acknowledge USGS and Deltares USA staff contributions to performing a detailed QA/QC procedure on the model results. Moreover, we want to thank everyone who provided a review of this paper, which substantially improved this manuscript. We also acknowledge significant computational support from the USGS high performance computing system (Falgout, n.d.).

References

Abeysirigunawardena, D. S., Gilleland, E., Bronaugh, D., and Wong, P.: Extreme wind regime responses to climate variability and change in the inner south coast of British Columbia, Canada, Atmosphere - Ocean, 47, 41–62, https://doi.org/10.3137/AO1003.2009, 2009.

Abeysirigunawardena, D. S., Smith, D. J., and Taylor, B.: Extreme Sea Surge Responses to Climate Variability in Coastal British Columbia, Canada, Annals of the Association of American Geographers, 101, 992–1010, 2011.

Barnard, P. L., van Ormondt, M., Erikson, L. H., Eshleman, J., Hapke, C., Ruggiero, P., Adams, P. N., and Foxgrover, A. C.: Development of the Coastal Storm Modeling System (CoSMoS) for predicting the impact of storms on high-energy, active-margin coasts, Natural Hazards, 74, 1095–1125, https://doi.org/10.1007/s11069-014-1236-y, 2014.

Barnard, P. L., Befus, K. M., Danielson, J. J., Engelstad, A. C., Erikson, L. H., Foxgrover, A. C., Hayden, M. K., Hoover, D. J., Leijnse, T. W. B., Massey, C., McCall, R., Nadal-Caraballo, N. C., Nederhoff, K., O'Neill, A. C., Parker, K. A., Shirzaei, M., Ohenhen, L. O., Swarzenski, P. W., Thomas, J. A., van Ormondt, M., Vitousek, S., Vos, K., Wood, N. J., Jones, J. M., and Jones, J. L.: Projections of multiple climate-related coastal hazards for the US Southeast Atlantic, Nat Clim Chang, https://doi.org/10.1038/s41558-024-02180-2, 2024.

Booij, N., Ris, R. C., and Holthuijsen, L. H.: A third-generation wave model for coastal regions 1. Model description and validation, J Geophys Res Oceans, 104, 7649–7666, https://doi.org/10.1029/98JC02622, 1999.

Brogli, R., Heim, C., Mensch, J., Sorland, S. L., and Schar, C.: The pseudo-global-warming (PGW) approach: Methodology, software package PGW4ERA5 v1.1, validation, and sensitivity analyses, Geosci Model Dev, 16, 907–926, https://doi.org/10.5194/gmd-16-907-2023, 2023.

https://doi.org/10.5194/egusphere-2026-3369
Preprint. Discussion started: 22 July 2026

Buitink, J., Dalmijn, B., Parker, K. A., Nederhoff, K., and Grossman, E.: Wetter Winters, Drier Summers: Quantifying the change in hydrological response around the Puget Sound area using the wflow_sbm hydrological model and CMIP6 projections, EarthArXiv, Preprint, https://doi.org/https://doi.org/10.31223/X58R0G, 2025.

Campos-Caba, R., Alessandri, J., Camus, P., Mazzino, A., Ferrari, F., Federico, I., Vousdoukas, M., Tondello, M., and Mentaschi, L.: Assessing storm surge model performance: what error indicators can measure the model's skill?, Ocean Science, 20, 1513–1526, https://doi.org/10.5194/os-20-1513-2024, 2024.

Cavaleri, L. and Bertotti, L.: The improvement of modelled wind and wave fields with increasing resolution, Ocean Engineering, 33, 553–565, https://doi.org/10.1016/j.oceaneng.2005.07.004, 2006.

Center for Operational Oceanographic Products and Services (CO-OPS), National Oceanic and Atmospheric Administration: NOS CO-OPS Water Level Data, Verified, 6-MinuteNOAA / NMFS SWFSC Environmental Research Division. Retrieved from https://coastwatch.pfeg.noaa.gov/erddap/tabledap/nosCoopsWLV6.html (2022, September 1).

Chen, H., Sun, J., Lin, W., and Xu, H.: Comparison of CMIP6 and CMIP5 models in simulating climate extremes, https://doi.org/10.1016/j.scib.2020.05.015, 15 September 2020.

Climate Impacts Group [CIG]: State of Knowledge: Climate Change in Puget Sound, https://doi.org/10.7915/CIG93777D, 2015.

Climate Impacts Group [CIG], U. of W.: Climate Change and Its effects on Puget Sound, 2005.

Cohen, J., Ye, H., and Jones, J.: Trends and variability in rain-on-snow events, Geophys Res Lett, 42, 7115–7122, https://doi.org/10.1002/2015GL065320, 2015.

Crosby, S. C., Nederhoff, C. M., VanArendonk, N., and Grossman, E. E.: Efficient modeling of wave generation and propagation in a semi-enclosed estuary, Ocean Model (Oxf), 184, https://doi.org/10.1016/j.ocemod.2023.102231, 2023.

Crosby, Sean C., and Eric Grossman.: Wave observations from nearshore bottom-mounted pressure sensors in Skagit and Bellingham Bays, Washington, USA from Dec 2017 to Feb 2018." *US Geological Survey (USGS) Data Release*. 2019

Environment and Climate Change Canada: The High Resolution Deterministic Prediction System (HRDPS) version 7.0.0 of the Meteorological Service of Canada (MSC), 2024.

Erikson, L., Barnard, P., O'Neill, A., Wood, N., Jones, J., Finzi Hart, J., Vitousek, S., Limber, P., Hayden, M., Fitzgibbon, M., Lovering, J., and Foxgrover, A.: Projected 21st Century Coastal Flooding in the

Southern California Bight. Part 2: Tools for Assessing Climate Change-Driven Coastal Hazards and Socio-Economic Impacts, J Mar Sci Eng, 6, 76, https://doi.org/10.3390/jmse6030076, 2018.

Eyring, V., Bony, S., Meehl, G. A., Senior, C. A., Stevens, B., Stouffer, R. J., and Taylor, K. E.: Overview of the Coupled Model Intercomparison Project Phase 6 (CMIP6) experimental design and organization, Geosci Model Dev, 9, 1937–1958, https://doi.org/10.5194/gmd-9-1937-2016, 2016.

Eyring, V., Cox, P. M., Flato, G. M., Gleckler, P. J., Abramowitz, G., Caldwell, P., Collins, W. D., Gier, B. K., Hall, A. D., Hoffman, F. M., Hurtt, G. C., Jahn, A., Jones, C. D., Klein, S. A., Krasting, J. P., Kwiatkowski, L., Lorenz, R., Maloney, E., Meehl, G. A., Pendergrass, A. G., Pincus, R., Ruane, A. C., Russell, J. L., Sanderson, B. M., Santer, B. D., Sherwood, S. C., Simpson, I. R., Stouffer, R. J., and Williamson, M. S.: Taking climate model evaluation to the next level, Nat Clim Chang, 9, 102–110, https://doi.org/10.1038/s41558-018-0355-y, 2019.

Falgout, Jeff T, Janice Gordon, Brad Williams, Matthew J. Davis, USGS Advanced Research Computing, USGS Denali Supercomputer: U.S. Geological Survey, https://doi.org/10.5066/P9PSW367, n.d.

Falgout, Jeff T, Janice Gordon, Lopaka Lee, Brad Williams, USGS Advanced Research Computing, USGS Hovenweep Supercomputer: U.S. Geological Survey, https://doi.org/10.5066/P927BI7R. n.d.

Gao, K., Harris, L., Chen, J. H., Lin, S. J., and Hazelton, A.: Improving AGCM Hurricane Structure With Two-Way Nesting, J Adv Model Earth Syst, 11, 278–292, https://doi.org/10.1029/2018MS001359, 2019.

Grossman, E. E., Tehranirad, B., Nederhoff, C. M., Crosby, S. C., Stevens, A. W., van Arendonk, N. R., Nowacki, D. J., Erikson, L. H., and Barnard, P. L.: Modeling Extreme Water Levels in the Salish Sea: The Importance of Including Remote Sea Level Anomalies for Application in Hydrodynamic Simulations, Water (Switzerland), 15, https://doi.org/10.3390/w15234167, 2023.

Grossman, E.E. and Crosby, S.C.: Wave observations from bottom-mounted pressure sensors along the West side of Whidbey Island, Washington from Dec 2018 to Jan 2020: U.S. Geological Survey data release, https://doi.org/10.5066/P907B0YM. 2024

Haarsma, R. J., Roberts, M. J., Vidale, P. L., Catherine, A., Bellucci, A., Bao, Q., Chang, P., Corti, S., Fučkar, N. S., Guemas, V., von Hardenberg, J., Hazeleger, W., Kodama, C., Koenigk, T., Leung, L. R., Lu, J., Luo, J. J., Mao, J., Mizielinski, M. S., Mizuta, R., Nobre, P., Satoh, M., Scoccimarro, E., Semmler, T., Small, J., and von Storch, J. S.: High Resolution Model Intercomparison Project (HighResMIP v1.0) for CMIP6, Geosci Model Dev, 9, 4185–4208, https://doi.org/10.5194/gmd-9-4185-2016, 2016.

Haiden, T., Janousek, M., Vitart, F., Ferranti, L., and Prates, F.: Evaluation of ECMWF forecasts, including the 2019 upgrade | ECMWF, 2019.

https://doi.org/10.5194/egusphere-2026-3369
Preprint. Discussion started: 22 July 2026

Hamman, J. J.: Effects of Projected Twenty-First Century Sea Level Rise, Storm Surge, and River Flooding on Water Levels in Puget Sound Floodplains and Estuaries, 2012.

Hermans, T. H. J., Busecke, J. J. M., Wahl, T., Malagón-Santos, V., Tadesse, M. G., Jane, R. A., and van de Wal, R. S. W.: Projecting Changes in the Drivers of Compound Flooding in Europe Using CMIP6 Models, Earths Future, 12, https://doi.org/10.1029/2023EF004188, 2024.

Hersbach, H., Bell, B., Berrisford, P., Biavati, G., Horányi, A., Muñoz Sabater, J., Nicolas, J., Peubey, C., Radu, R., Rozum, I., Schepers, D., Simmons, A., Soci, C., Dee, D., Thépaut, J.-N.: ERA5 hourly data on single levels from 1940 to present, Copernicus Climate Change Service (C3S) Climate Data Store (CDS), https://doi.org/10.24381/cds.adbb2d47, 2023.

Idier, D., Bertin, X., Thompson, P., and Pickering, M. D.: Interactions Between Mean Sea Level , Tide , Surge , Waves and Flooding : Mechanisms and Contributions to Sea Level Variations at the Coast, Surv Geophys, 40, 1603–1630, https://doi.org/10.1007/s10712-019-09549-5, 2019.

Intergovernmental Panel on Climate Change (IPCC): Climate Change 2021: The Physical Science Basis. Contribution of Working Group I to the Sixth Assessment Report of the Intergovernmental Panel on Climate Change. [Masson-Delmotte, V., P. Zhai, A. Pirani, S.L. Connors, C. Péan, S. Berger, N. Caud, Y. Chen, L. Goldfarb, M.I. Gomis, M. Huang, K. Leitzell, E. Lonnoy, J.B.R. Matthews, T.K. Maycock, T. Waterfield, O. Yelekçi, R. Yu, and B. Zhou (eds.)]. Cambridge University Press, Cambridge, United Kingdom and New York, NY, USA, In press, doi:10.1017/9781009157896. 2021

Intergovernmental Panel on Climate Change (IPCC): Future Global Climate: Scenario-based Projections and Near-term Information, in: Climate Change 2021 – The Physical Science Basis, Cambridge University Press, 553–672, https://doi.org/10.1017/9781009157896.006, 2023.

Katzenberger, A., Perez-Carrasquilla, J. S., Gemmell, K., Galytska, E., Leclerc, C., Punya, P., Roy, I., Varuolo-Clarke, A., Tošić, M., and Črnivec, N.: Developing Guidelines for Working with Multi-Model Ensembles in CMIP, https://doi.org/10.5194/egusphere-2025-4744, 6 October 2025.

Kernkamp, H. W. J., van Dam, A., Stelling, G. S., and de Goede, E. D.: Efficient scheme for the shallow water equations on unstructured grids with application to the Continental Shelf, Ocean Dyn, 61, 1175–1188, https://doi.org/10.1007/s10236-011-0423-6, 2011.

King County: WRIA 9 Marine Shoreline Monitoring and Compliance Project Phase 2 Final Report. Prepared by Kollin Higgins, King County Water and Land Resources Division, Science and Technical Support Section. Seattle, Washington. 2019

Komen, G. J. L. C. M. D. K. H. S. H. and P. A. E. M. J.: Dynamics and modelling of ocean waves , Cambridge university press, Cambridge, UK, 1994.

https://doi.org/10.5194/egusphere-2026-3369
Preprint. Discussion started: 22 July 2026

Lyard, F. H., Allain, D. J., Cancet, M., Carrère, L., and Picot, N.: FES2014 global ocean tide atlas: Design and performance, Ocean Science, 17, 615–649, https://doi.org/10.5194/os-17-615-2021, 2021.

MacCready, P. and Geyer, W. R.: Estuarine Exchange Flow in the Salish Sea, J Geophys Res Oceans, 129, https://doi.org/10.1029/2023JC020369, 2024.

Makkonen, L.: Plotting Positions in Extreme Value Analysis, J Appl Meteorol Climatol, 45, 334–340, https://doi.org/https://doi.org/10.1175/JAM2349.1, 2006.

McMichael, C., Dasgupta, S., Ayeb-Karlsson, S., and Kelman, I.: A review of estimating population exposure to sea-level rise and the relevance for migration, https://doi.org/10.1088/1748-9326/abb398, 1 December 2020.

Meehl, G. A., Senior, C. A., Eyring, V., Flato, G., Lamarque, J.-F., Stouffer, R. J., Taylor, K. E., and Schlund, M.: Context for interpreting equilibrium climate sensitivity and transient climate response from the CMIP6 Earth system models, 2020.

Miller, I., Morgan, H., Mauger, G., Weldon, R., Schmidt, D., Welch, M., and Grossman, E.: PROJECTED SEA LEVEL RISE for WASHINGTON STATE A 2018 ASSESSMENT Projected Sea Level Rise for Washington State, Washington Coastal Resilience Project, 2018.

Mofjeld, H. O. and Larsen, L. H.: TIDES AND TIDAL CURRENTS OF THE INLAND WATERS OF WESTERN WASHINGTON, 1984.

Muis, S., Aerts, J. C. J. H., José, J. A., Dullaart, J. C., Duong, T. M., Erikson, L., Haarsma, R. J., Apecechea, M. I., Mengel, M., le Bars, D., O'Neill, A., Ranasinghe, R., Roberts, M. J., Verlaan, M., Ward, P. J., and Yan, K.: Global Projections of Storm Surges Using High-Resolution CMIP6 Climate Models, Earths Future, 11, https://doi.org/10.1029/2023EF003479, 2023.

Nederhoff, K., Parker, K., and Grossman, E.: Beyond the 100-Year Flood: Probabilistic Flood Hazard Assessment for King and Pierce Counties under Future Climate Scenarios, EGUsphere [preprint], https://doi.org/10.5194/egusphere-2025-4909, 2025.

National Data Buoy Center (NDBC): Wave Observations. NOAA., from https://www.ndbc.noaa.gov. 2022

Nowacki, C.J., Vanarendonk, N.R., Stevens, A., Grossman, E., and Tan, A.CML.: Oceanographic and water-quality measurements collected in Bellingham Bay, Washington, USA, 2019 to 2021: U.S. Geological Survey data release, https://doi.org/10.5066/P96EH1MS. 2023

Olabarrieta, M., Warner, J. C., and Kumar, N.: Wave-current interaction in Willapa Bay, J Geophys Res, 116, C12014, https://doi.org/10.1029/2011JC007387, 2011.

Parker, K. and Hill, D. F.: Evaluation of bias correction methods for wave modeling output, Ocean Model (Oxf), 110, 52–65, https://doi.org/10.1016/j.ocemod.2016.12.008, 2017.

Parker, K., Nederhoff, K., Engelstad, A., Grossman, E., Erikson, L., and Crosby, S: Water level and wave heights for Salish Sea Coastal Storm Modeling System, U.S. Geological Survey data release, https:/doi.org/10.5066/P14VOPEY/. 2026

Rivas, M. B. and Stoffelen, A.: Characterizing ERA-Interim and ERA5 surface wind biases using ASCAT, 831–852, 2019.

Roberts, M. J., Baker, A., Blockley, E. W., Calvert, D., Coward, A., Hewitt, H. T., Jackson, L. C., Kuhlbrodt, T., Mathiot, P., Roberts, C. D., Schiemann, R., Seddon, J., Vannière, B., and Luigi Vidale, P.: Description of the resolution hierarchy of the global coupled HadGEM3-GC3.1 model as used in CMIP6 HighResMIP experiments, Geosci Model Dev, 12, 4999–5028, https://doi.org/10.5194/gmd-12-4999-2019, 2019.

Ruggiero, P., Komar, P. D., and Allan, J. C.: Increasing wave heights and extreme value projections: The wave climate of the U.S. Pacific Northwest, Coastal Engineering, 57, 539–552, https://doi.org/10.1016/j.coastaleng.2009.12.005, 2010.

Shipman, H., Gelfenbaum, G., Dethier, M. N., and Fresh, K. L.: Puget Sound Shoreline Armoring: State of the Science Workshop, n.d. 2010.

Simenstad, C. A., Ramirez, M., Burke, J., Logsdon, M., Shipman, H., Tanner, C., Toft, J., Craig, B., Davis, C., Fung, J., Bloch, P., Fresh, K., Campbell, S., Myers, D., Iverson, E., Bailey, A., Schlenger, P., Kiblinger, C., Myre, P., … MacLennan, A. Historical change of Puget Sound shorelines: Puget Sound nearshore ecosystem project change analysis. (Report No. 2011-01). Washington Department of Fish and Wildlife & U.S. Army Corps of Engineers, 2011

Sobocinski, K.L.: State of the Salish Sea, G. Broadhurst and N.J.K. Baloy (Contributing Eds.). Salish Sea Institute, Western Washington University. https://doi.org/10.25710/vfhb-3a69, 2021.

Soci, C., Hersbach, H., Simmons, A., Poli, P., Bell, B., Berrisford, P., Horányi, A., Muñoz-Sabater, J., Nicolas, J., Radu, R., Schepers, D., Villaume, S., Haimberger, L., Woollen, J., Buontempo, C., and Thépaut, J. N.: The ERA5 global reanalysis from 1940 to 2022, Quarterly Journal of the Royal Meteorological Society, https://doi.org/10.1002/qj.4803, 2024.

Solbrekke, I. M., Sorteberg, A., and Haakenstad, H.: The 3 km Norwegian reanalysis (NORA3)-a validation of offshore wind resources in the North Sea and the Norwegian Sea, Wind Energy Science, 6, 1501–1519, https://doi.org/10.5194/wes-6-1501-2021, 2021.

Soontiens, N., Allen, S. E., Latornell, D., le Souëf, K., MacHuca, I., Paquin, J. P., Lu, Y., Thompson, K., and Korabel, V.: Storm Surges in the Strait of Georgia Simulated with a Regional Model, Atmosphere - Ocean, 54, 1–21, https://doi.org/10.1080/07055900.2015.1108899, 2016.

Stevens, A. W. and Lacy, J. R.: The Influence of Wave Energy and Sediment Transport on Seagrass Distribution, 35, 92–108, https://doi.org/10.1007/s, 2012.

Stevens, A. W., Ruggiero, P., Parker, K. A., Vitousek, S., Gelfenbaum, G., and Kaminsky, G. M.: Climate controls on longshore sediment transport and coastal morphology adjacent to engineered inlets, Coastal Engineering, 194, https://doi.org/10.1016/j.coastaleng.2024.104617, 2024.

Sweet, W. V., Hamlington, B. D., Kopp, R. E., Weaver, C. P., Barnard, P. L., Bekaert, D., Brooks, W., Craghan, M., Dusek, G., Frederikse, T., Garner, G., Genz, A. S., Krasting, J. P., Larour, E., Marcy, D., Marra, J. J., Obeysekera, J., Osler, M., Pendleton, M., Roman, D., Schmied, L., Veatch, W., White, K. D., and Zuzak, C.: Global and Regional Sea Level Rise Scenarios for the United States: Updated Mean Projections and Extreme Water Level Probabilities Along U.S. Coastlines, Silver Spring, MD, 111 pp. pp., 2022.

Tebaldi, C., Debeire, K., Eyring, V., Fischer, E., Fyfe, J., Friedlingstein, P., Knutti, R., Lowe, J., O'Neill, B., Sanderson, B., van Vuuren, D., Riahi, K., Meinshausen, M., Nicholls, Z., Tokarska, K., Hurtt, G., Kriegler, E., Meehl, G., Moss, R., Bauer, S., Boucher, O., Brovkin, V., Yhb, Y., Dix, M., Gualdi, S., Guo, H., John, J., Kharin, S., Kim, Y. H., Koshiro, T., Ma, L., Olivié, D., Panickal, S., Qiao, F., Rong, X., Rosenbloom, N., Schupfner, M., Séférian, R., Sellar, A., Semmler, T., Shi, X., Song, Z., Steger, C., Stouffer, R., Swart, N., Tachiiri, K., Tang, Q., Tatebe, H., Voldoire, A., Volodin, E., Wyser, K., Xin, X., Yang, S., Yu, Y., and Ziehn, T.: Climate model projections from the Scenario Model Intercomparison Project (ScenarioMIP) of CMIP6, Earth System Dynamics, 12, 253–293, https://doi.org/10.5194/esd-12-253-2021, 2021.

Thomson, R. E., Rabinovich, A. B., Fine, I. v., Sinnott, D. C., McCarthy, A., Sutherland, N. A. S., and Neil, L. K.: Meteorological tsunamis on the coasts of British Columbia and Washington, Physics and Chemistry of the Earth, 34, 971–988, https://doi.org/10.1016/j.pce.2009.10.003, 2009.

Timmermans, B. W., Gommenginger, C. P., Dodet, G., and Bidlot, J. R.: Global Wave Height Trends and Variability from New Multimission Satellite Altimeter Products, Reanalyses, and Wave Buoys, Geophys Res Lett, 47, https://doi.org/10.1029/2019GL086880, 2020.

Vousdoukas, M. I., Mentaschi, L., Voukouvalas, E., Verlaan, M., Jevrejeva, S., Jackson, L. P., and Feyen, L.: Global probabilistic projections of extreme sea levels show intensification of coastal flood hazard, Nat Commun, 9, https://doi.org/10.1038/s41467-018-04692-w, 2018.

https://doi.org/10.5194/egusphere-2026-3369
Preprint. Discussion started: 22 July 2026

Walker, S., Mozaria-Luna, H. N., Kaplan, I., and Petatán-Ramírez, D.: Future temperature and salinity in Puget Sound, Washington State, under CMIP6 climate change scenarios, Journal of Water and Climate Change, 13, 4255–4272, https://doi.org/10.2166/wcc.2022.282, 2022.

World Meteorological Organization: WMO Guidelines on the Calculation of Climate Normals, WMO-No. 1203, 2017.

Yang, Z., García-Medina, G., Wu, W.-C., Wang, T., Ruby, L., Castrucci, L., and Mauger, G.: Modeling Analysis of the Swell and Wind-Sea Climate in the Salish Sea, Estuar Coast Shelf Sci, 289–300, 2019.

Yang, Z., Wang, T., Castrucci, L., and Miller, I.: Modeling assessment of storm surge in the Salish Sea, Estuar Coast Shelf Sci, 238, 2020.

Appendix A: Model Validation

A brief summary of model validation information is provided here. Table A1 details model performance of modeled water levels compared against tide gauge data at all locations within the model domain. Comparison is for the full period of overlap of the reanalysis model period (1940–2023) and tide gauge data availability (6-min validated data, Center for Operational Oceanographic Products and Services, 2022). Model skill metrics are shown for still water levels, non-tidal residuals (NTR), and tides. NTR were calculated for model results by subtracting a tide-only simulation (no forcing other than astronomical tides) from a simulation with full forcing applied. NTR were calculated for tide gauge data by subtracting the observed water level from the NOAA predicted tide timeseries (Center for Operational Oceanographic Products and Services (CO-OPS), 2022).

Metrics are defined as follows:

- RMSE: Root Mean Square Error
- R^2: Coefficient of Determination
- MADc: Corrected Mean Absolute Deviation (phase-error resistant metric proposed by Campos-Caba et al., 2024)
- Bias: Bias
- Slope: Slope of the linear fit between observations and the simulation.

https://doi.org/10.5194/egusphere-2026-3369
Preprint. Discussion started: 22 July 2026

Table A1: Model Performance at Tide Gauges across the Salish Sea

Water Levels

Gauge	Location	Record Length (yrs)	RMSE	R^2	MADc	AbsBias	Slope
9443090	Neah Bay	27.6	0.133	0.968	0.122	0.047	0.990
9444090	Port Angeles	27.0	0.137	0.963	0.362	0.004	0.905
9444900	Port Townsend	27.6	0.163	0.963	0.362	-0.059	0.907
9447130	Seattle	28.1	0.131	0.985	0.177	-0.014	0.972
9446484	Tacoma	26.1	0.132	0.986	0.137	0.016	0.976
9449880	Friday Harbor	27.6	0.141	0.967	0.140	0.061	0.972
9449424	Cherry Point	27.4	0.132	0.978	0.218	-0.042	0.978
Average	----------------		0.138	0.973	0.217	0.002	0.959

Non-Tidal Residual

Gauge	Location		RMSE	R^2	MADc	AbsBias	Slope
9443090	Neah Bay	27.6	0.135	0.197	0.161	-0.041	0.904
9444090	Port Angeles	27.0	0.124	0.270	0.107	-0.003	0.923
9444900	Port Townsend	27.6	0.130	0.090	0.143	0.023	0.929
9447130	Seattle	28.1	0.138	0.010	0.139	0.033	0.845
9446484	Tacoma	26.1	0.138	0.001	0.139	0.035	0.839
9449880	Friday Harbor	27.6	0.125	0.162	0.130	0.015	1.006
9449424	Cherry Point	27.4	0.123	0.240	0.113	-0.011	0.967
Average	----------------		0.113	0.138	0.133	0.009	0.916

Tides

Gauge	Location		RMSE	R^2	MADc	AbsBias	Slope
9443090	Neah Bay	27.6	0.145	0.962	0.143	0.089	0.974
9444090	Port Angeles	27.0	0.127	0.966	0.327	0.005	0.895
9444900	Port Townsend	27.6	0.164	0.962	0.431	-0.082	0.897
9447130	Seattle	28.1	0.115	0.988	0.228	-0.048	0.967
9446484	Tacoma	26.1	0.102	0.991	0.176	-0.019	0.977
9449880	Friday Harbor	27.6	0.121	0.975	0.175	0.046	0.964
9449424	Cherry Point	27.4	0.129	0.978	0.235	-0.031	0.974
Average	----------------		0.129	0.975	0.245	-0.006	0.950

https://doi.org/10.5194/egusphere-2026-3369
Preprint. Discussion started: 22 July 2026

Similar data are provided here comparing modeled significant wave heights and periods to available observations (National Data Buoy Center, 2022, Grossman et al., 2024, Nowacki et al., 2023, Crosby and Grossman, 2019):

1030

Table A2: Model Performance at wave observation points across the Salish Sea

Significant Wave Height

Location	Type	Record Length (days)	RMSE	R^2	MADc	Bias	Slope
Angeles Point	NDBC Buoy (Station 46267)	929	0.34	0.13	0.35	0.19	0.57
Bellingham Bay 1	Pressure Sensor	106	0.17	0.34	0.15	0	0.62
Bellingham Bay 3	Pressure Sensor	198	0.17	0.57	0.15	0.05	0.62
Bellingham Bay 4	Pressure Sensor	78	0.18	0.62	0.16	-0.04	0.73
Halibut Bank	NDBC Buoy (Station 46146)	9923	0.28	0.08	0.25	-0.07	0.96
Hein Bank	NDBC Buoy (Station 46088)	6833	0.28	0.36	0.23	-0.01	1.02
S1	Pressure Sensor	60	0.12	0.59	0.12	0	0.58
S2	Pressure Sensor	60	0.13	0.58	0.11	-0.01	0.53
S3	Pressure Sensor	41	0.11	0.16	0.11	-0.04	0.44
Spotter	Buoy	569	0.13	0.65	0.12	0	0.92
W1	Pressure Sensor	131	0.22	0.37	0.16	0.09	0.38
W2	Pressure Sensor	131	0.23	0.41	0.16	0.09	0.42
W3	Pressure Sensor	135	0.33	0.02	0.26	0.21	0.33
W4	Pressure Sensor	135	0.28	-0.01	0.24	0.18	0.4
W5	Pressure Sensor	145	0.32	0.22	0.26	0.18	0.49
W7	Pressure Sensor	142	0.2	0.51	0.15	0.11	0.53
Average	----------------		0.22	0.35	0.19	0.06	0.60

Mean Wave Period

Gauge	Location	RMSE	R^2	MADc	AbsBias	Slope

https://doi.org/10.5194/egusphere-2026-3369
Preprint. Discussion started: 22 July 2026

Angeles Point	NDBC Buoy (Station 46267)	929	2.39	-0.65	3.19	1.25	0.68
Bellingham Bay 1	Pressure Sensor	106	0.77	-6.18	1.55	0.6	0.34
Bellingham Bay 3	Pressure Sensor	198	0.78	-5.63	1.49	0.68	0.73
Bellingham Bay 4	Pressure Sensor	78	0.69	-1.23	1.35	0.58	0.8
Hein Bank	NDBC Buoy (Station 46088)	6833	1.98	-3.17	2.67	1.58	0.08
S1	Pressure Sensor	60	0.41	-2.39	0.72	0.29	0.65
S2	Pressure Sensor	60	0.4	-4.37	0.7	0.31	0.92
S3	Pressure Sensor	41	0.6	-6.21	0.96	0.55	0.43
Spotter	Buoy	569	0.74	-2.06	1.23	0.64	0.83
W1	Pressure Sensor	131	2.06	-2.8	2.51	1.69	-0.05
W2	Pressure Sensor	131	3.01	-3.11	3.69	2.54	-0.04
W3	Pressure Sensor	135	1.96	-5.86	2.89	1.74	-0.05
W4	Pressure Sensor	135	2.21	-4.42	3.05	1.92	-0.04
W5	Pressure Sensor	145	2.34	-4.64	3.21	1.98	-0.11
W7	Pressure Sensor	142	2.76	-2.42	2.93	2.2	-0.03
Average	----------------		1.54	-3.68	2.14	1.24	0.34